# *ANALYSIS OF A LARGE SCALE SOLAR WATER HEATER*

by

PAUL M. RATZMANN

A thesis submitted in partial fulfillment

of the requirements for the degree of

**MASTER OF SCIENCE**

(Mechanical Engineering)

at the

**UNIVERSITY OF WISCONSIN -- MADISON**

1992

# CHAPTER ONE

## INTRODUCTION

Packerland Solar System, located in Green Bay, WI, provides hot water for the Packerland Meat Packing Company. The system consists of 5256 solar collectors connected in a series-parallel arrangement. The primary goal of this project is to obtain an accurate computer model of the system with the intent to establish the system efficiency and recommend economically feasible changes to improve system design and operation.

### 1.1 PROJECT DESCRIPTION AND GOAL

The computer model used is TRNSYS (Transient System Analysis) Version 13.1 [1] developed at the UW-Madison Solar Energy Laboratory. TRNSYS provides a library of HVAC and solar equipment components which may be connected in a wide variety of system configurations. The components are built in the simulation program in much the same way as the actual hardware. Inputs and outputs in each component of the simulation are in the form of information flow and parallel flow in the real system.

The two phases of this project are the data acquisition and the simulation model development and use. Using solar data acquired from the actual system, the computer model is developed to match actual energy output. Once system parameters have been established, changes may then be made to the parameters of the computer model to determine their effect on performance and predict how these changes may affect the system.

In the large banks of collectors such as those located at Packerland, some of the collectors may experience a low rate of flow, and others experience a high rate. The problem of poor flow distribution results in a drop in performance which has been investigated computationally and verified experimentally. It is possible to quantify the effect of this poor distribution on both individual banks of collectors and on the system as a whole. Three methods for determining the flow distribution in collector banks have been considered, two of which have been carried out and evaluated.

Chapter One describes the Packerland system components and a short history of the system. Chapter Two covers the problem of flow distribution and presents the results of the study, as well as a more general solution to the problem to be applied to other systems of collectors. The limitations of both methods used to determine the flow distribution are provided as well.

During a two week period data acquisition took place. Chapter Three discusses the equipment used and also provides diagrams of the system where sensors were located for the recording of data. Chapter Four covers simulation results provided by both an $f$-Chart [8] and TRNSYS [1] analysis. Methods of determining pertinent parameters such as flow rates and loss coefficients are discussed here.

Slight alterations in the hardware and control strategy could result in significant increases in the annual energy output of Packerland Solar System. Chapter Five presents the results of the study and provides recommendations which could achieve this predicted improvement in performance, as well as a short discussion on the direction of future work.

## 1.2 THE PACKERLAND SYSTEM

The Packerland system is composed of 5256 collectors connected in a series-parallel arrangement. Each collector has 31.5 square feet of gross area yielding a total collector area of 165564 square feet. The working fluid is a water/propylene glycol mix pumped through the array with four 15 horsepower pumps. During the warm months the replacement fluid is water and during the cold months it is glycol resulting in a variation of mixture percentage between about 35 to 65 percent propylene glycol throughout the year.

The amount of energy provided to the plant from the Packerland system is calculated at the plant by the use of an Energy meter. The Energy meter is a recording device which takes the mass flow rate of the water drawn from the tank over a 15 minute period and uses the average temperature increase of the water over that of the city water to calculate the energy provided by the solar system. The device prints out on hard copy the 15 minute, one hour and

24 hour totals of water pumped and energy provided for each day of operation (see Figure 1.2.1).

The solar heated water is distributed to five different heat exchangers that operate at temperatures of 90, 95, 118, 150, and 180°F. If water supplied from the tank is below the set temperature, steam is input to the heat exchanger to bring the water up to temperature. If the tank water is too warm, it is brought down to temperature by mixing with cold supply water [13]. Although this load information is not used for modeling purposes, it is provided here as a matter of completeness.

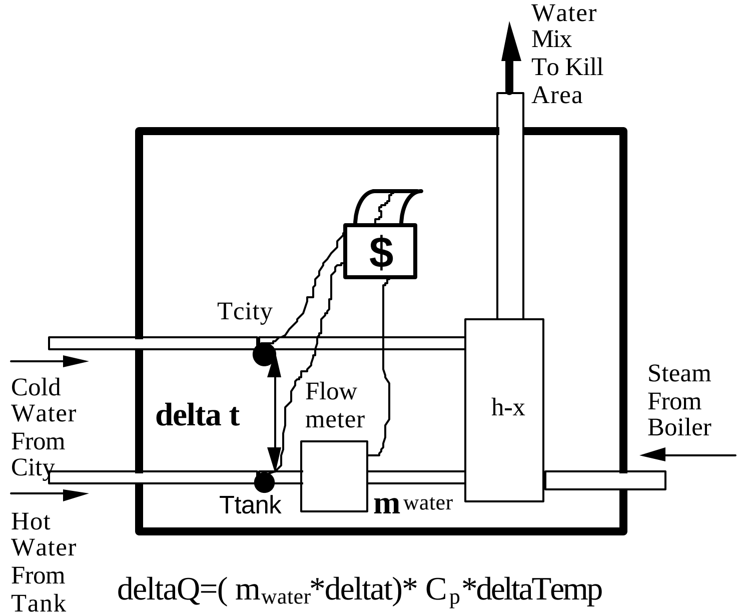


**Figure 1.2.1 In Plant Energy Monitoring**

The heated glycol is sent into a heat exchanger manufactured by Alfa Laval, Inc. located in Fort Lee, NJ. It is a plate heat exchanger consisting of a number of heat transfer plates, arranged so that every other passage between the plates is accessible for one of two liquids

[2]. The UA of the heat exchanger has been found to be 609000 Btu/hr-°F and is assumed constant at this value for all analyses except during the sensitivity simulations in Chapter 4. Since the water from the tank is required to be potable, there is an inner water loop in the heat exchanger to ensure that the potable water is not contaminated by the glycol (see Figure 1.2.3).

The Model SS-12 flat plate collector was manufactured by Solar King based in Waco, TX. One of the collectors was sent to the **Florida Solar Energy Center** in 1985 to be tested in accordance with ASHRAE Standard 93-77 [3]. Both a linear and quadratic model of efficiency were provided by the test. The test flow rate was 0.85 GPM and the working fluid was water. Pressure drop in the collector under test conditions was 0.12 PSI. The linear model was chosen for its simplicity of use in both *f*-Chart and TRNSYS. The linear parameters determined from the test are provided below. Additional collector information is provided in detail in the Appendix.

**Figure 1.2.2 Model SS-12 Solar King Flat Plate Collector**

The storage tank is 41 feet tall and 38 feet in diameter. It has a capacity of 330000 gallons. During day to day operation of the system the tank level is varied between about 25 feet to 37 feet throughout the day depending on the control strategy and the draw of water from the tank, and is sometime drawn down to a minimum of 12 feet. The bottom, top and sides of the tank are insulated by either foam or fiberglass. The bottom has 2 inches of foam, the top 3 inches of sprayed foam, and the sides 3 inches of fiberglass. The thermal conductivity of all tank insulation is assumed to be 0.023 . All material information will later be used to estimate the tank losses for the TRNSYS model.

Return water from the heat exchanger is pumped into the top of the tank, and when water is drawn from the tank to the heat exchanger, it is drawn from the tank bottom. The load water drawn from the meat packing plant is drawn from the tank bottom as well. Although an unusual design for a solar collector system, it has been operating as such since being refurbished in 1987. Normal operation of a solar collector system will draw water from the tank top to enhance temperature stratification within the tank. The hot water will always go to the load and the cold water to the heat exchanger.

Originally the system was designed to draw the load from the top of the tank, but was redesigned with the current piping to enable variation of the tank level throughout the day [12]. The affect of this design change will be evaluated and discussed later in Chapter Four.

City (or supply) water is pumped out of Lake Michigan and is considerably colder than the ambient temperature during summer months. It is generally available at temperatures of 35 to 50 °F throughout the year.

The control scheme is designed to operate the optimum number of pumps during the day. When the sun first begins shining on the collector array, the first glycol pump is turned on. When the glycol is warm, the remaining glycol pumps are turned on and remain so for the rest of the day. The middle loop and tank loop pumps operate under a complicated scheme. During low levels of solar radiation, one or two of these pumps will be turned on, the number being determined by the temperature difference of the glycol across the heat exchanger. When the temperature difference exceeds 13 °F, the next pump will turn on until all pumps are on [12].

The pumping set up is shown in Figure 1.2.3. The glycol loop has four pumps, three of which are in parallel. The bank of three pumps is again in parallel with the fourth pump. This arrangement of glycol pumps is the result of a design flaw built into the original system [12]. The total glycol flow rate has been found to be 1250 GPM. The middle and tank water loops are each pumped by three 10 horsepower pumps in parallel and are controlled by the method described above. The flow rate in the middle loop of the heat exchanger has not been determined because of the complexity of this consideration, and due to the lack of available information provided about the heat transfer characteristics of the heat exchanger by the manufacturer. The flow rate between the tank and the heat exchanger varies due to the number of pumps operating, and if the supply water is being pumped through or not. The approximate flow rate of the water on the tank side was found to be about 4500 GPM.

**Figure 1.2.3 Pumping Setup**

Another portion of the control scheme is carried out by varying the tank level throughout the day. Quite often the tank level is drawn down during the night, and if the tank level remains above 12 feet, no replacement water will be pumped in. In the morning the tank is less than full so that when the sun first shines on the array, the cold city water is directly pumped into the heat exchanger and goes to fill the tank even before the meat packing plant begins the daily draw. At the end of the day the same type of scheme is followed. The tank level is drawn down from the meat packing plant with no replacement water and the remaining energy in the glycol is removed via the heat exchanger by again pumping cold city water directly into the heat exchanger. The tank is filled again with energy from the glycol even though there is no remaining solar insolation. During weekends and holidays when the meat packing plant does not operate, the tank is first filled with city water through the heat exchanger and continues to operate by drawing water from the tank.

The goal of this operational scheme is to maintain the lowest temperature on the water side into the heat exchanger. Variation of the tank level enables operation of the system beginning earlier in the morning and operating later into the evening than if the water into the heat exchanger were from the tank alone. This unique method of control is the reason the system was redesigned to draw the load from the tank bottom. It will be evaluated and compared to a more traditional mode of operation later in Chapter Four.

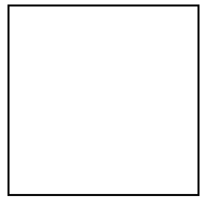

**Figure 1.2.4 The Packerland System**

The Packerland System originally came on line in 1983 with 9750 collectors, but due to initial design problems it was shut down in 1985. The system was dismantled and rebuilt at its current size in the fall of 1987. It has been successfully providing energy to Packerland Meat Packing since then. In Figure 1.2.5 is a summary of the energy provided since coming on line [13].

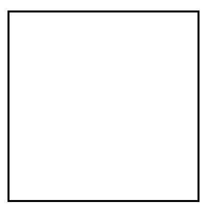

**Figure 1.2.5 Packerland Energy Output**

# CHAPTER TWO

## FLOW DISTRIBUTION

When solar collectors are connected in parallel, the flow rate near the outer collectors is increased while the flow rate near the center decreases. If the bank is large enough this poor distribution of flow will result, to a certain extent, in a deterioration of performance in the entire bank. Three methods of solution to determine the flow distribution are presented, two of which are used to evaluate the flow. The flow distribution is determined for a variety of flow rates and the resulting drop in performance is quantified and compared to an ideal calculation of performance were the flow to be evenly distributed.

## 2.1 THE PACKERLAND FLOW SYSTEM

The Packerland System collector array is broken up into three smaller banks which are fed by a main piping system from the heat exchanger. Each of these arrays is fed by an 8 inch diameter line with an 8 inch return to the heat exchanger. Along these feed lines are smaller taps which go to banks of either 108 or 180 collectors. All collector arrays are six high as shown in the figure below. Cool glycol comes in through the main feed line, is heated in the large banks and exits the bank to the large return line which sends the hot glycol to the heat exchanger. 1890 of the 5256 total collectors in the system are connected in banks of 15 wide. Each line off of the main feed goes to two banks (one of which is shown below) of either 15 wide or 9 wide. A few of the collector banks in the array are not exactly 9 or 15 across but the majority are connected as such.

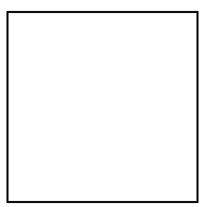

**Figure 2.1.1 Collector Bank of 15**

The flow of glycol enters at the bottom of rows one through six and exits through the top of each row on the other side of the bank. The method of feeding through the bottom of the array ensures that any air which enters the system will flow to the top and may be removed by way of an air release valve. It also simplifies filling the empty array sections with glycol after maintenance.

The Packerland system collectors each have 17 risers, so for one bank of 15 collectors there are a total of 255 risers drawn off of the lower header. All collector banks are tilted to 45° off of the horizontal.

## 2.2 FLOW IN LARGE BANKS

A solar collector is tested under ASHRAE 93-77 [3] to evaluate the operating parameters of flat plate collectors. Equations 2.1 and 2.2 describe the effect of varying the mass flow rate or the specific heat of the operating fluid. According to Equation 2.1 there are essentially two parameters which will cause the collector to operate differently than found in the ASHRAE standard. They are the fluid flow rate and the specific heat of the fluid. By operating the collector under different than test conditions, a correction must be calculated with Equation 2.1 then applied to the collector efficiency parameters using Equation 2.2 [4]. These two variables are and which appear in the numerator of 2.1.

(2.1)

(2.2)

The mass flow rate in a bank of collectors is not necessarily sufficient information to determine the average flow rate in each collector. When so many collectors are connected in parallel it may be necessary to determine the average flow rate of the glycol in each collector, and quantify its affect on the system performance with Equation 2.1. In general, a set of risers connected as such results in a high rate of flow in the outer (far left and far right) risers, and the flow rate near the center of the bank is very low. If the flow rate in the center collectors is too low, the temperature in these collectors will become excessive resulting in high thermal losses. A part of this project has been devoted to determining a general approach to find the flow rate throughout the bank, and present the effect of poor flow distribution on system performance. This approach has been used on the Packerland system for both bank types of 9 and 15 collectors.

The flow distribution problem has been verified for the Packerland system experimentally. Using a hand held radiometer manufactured**Error!**

Since the radiometer was calibrated with water, the absolute temperatures of the collector surface is not expected to be correct. The emissivity of water is high, as is the emissivity of the collector cover, but they are not identical. Without carrying out corrections for the different emissivities the relative temperatures are expected to yield accurate results, and the trend in Figure 2.2.1 is apparent. The higher temperatures near the center are an indication of a low flow rate with the reverse true near the outer collectors. Figures 2.2.1 and 2.2.2 were taken on the same collector bank on the first and third collectors from the bottom (see Figure 2.1.1).

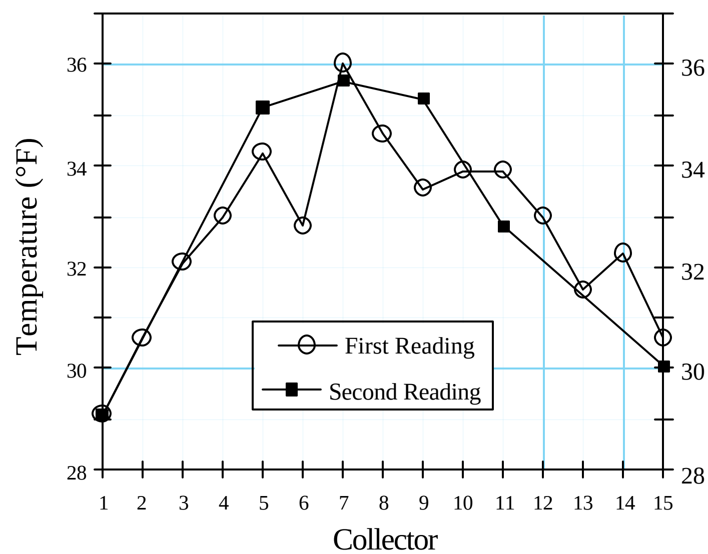


**Figure 2.2.1 Bottom Collector Surface Temperature**

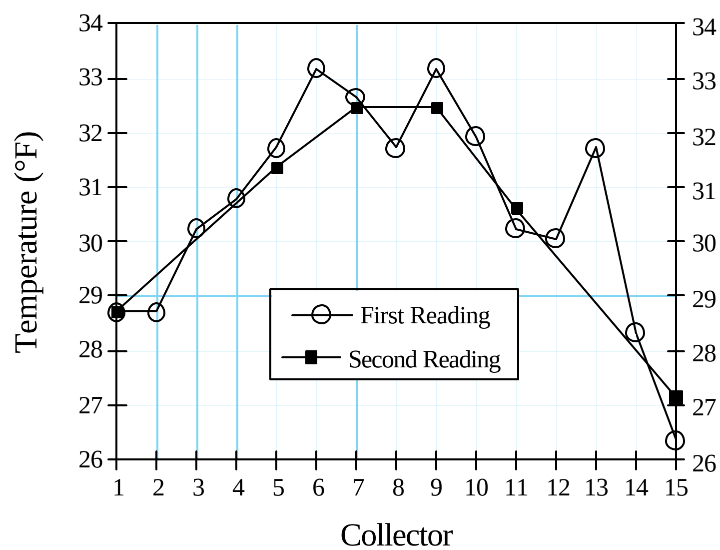

**Figure 2.2.2 Third From Bottom Collector Surface Temperature**

Three approaches to determine the flow rate in each individual collector have been taken. The first approach considered is an analytical solution which was presented at the 1970 International Solar Energy Society Conference by Dunkle and Davey [6]. Another approach was taken as described by Hirsch [5] and expanded upon. A program written by the National Renewable Energy Laboratory (NREL, previously known as the Solar Energy Research Institute, SERI) was also made available for this project which does the same [13]. The following section describes the approach to each, how they differ, and the last two sections describe the results of the study.

## 2.3 THREE APPROACHES

### Dunkle and Davey

An analytical solution to the problem of poor flow distribution in large banks of flat plate collectors was presented by Dunkle and Davey [6]. The method was applied for the Packerland Bank of collectors, but was found to yield results considerably off from those in both the NREL and Pipe Flow Analysis (PFA) solutions. The problem is solved by replacing the separate risers in the array by a distributed flow resistance between the headers. The flow varies continuously along the headers rather than in a series of steps corresponding to the flow in each riser.

Assuming the flow is turbulent in the headers and laminar in the risers, a series of equations is presented which describe both the flow distribution and the pressure variation within the bank. The numerical results presented in the following section indicate the flow in the risers is really turbulent, hence the assumption of laminar flow in the Dunkle and Davey solution does not hold. The article is mentioned here only as a matter of completeness.

**Pipe Flow Analysis (PFA) Solution**

A method for determining the flow distribution in banks of flat plate collectors was reported by Hirsch [5]. The energy equation for pipe flow is written for each riser between the upper and lower headers and yields the following equations which describe pressure drop and fluid velocity in the riser [18]:

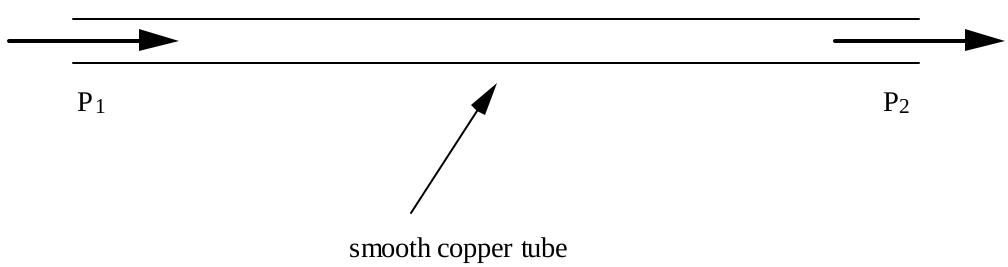


**Figure 2.3.1 Pressure Drop in Copper Tube Riser**

$$\Delta P = f \frac{L}{D} \frac{\rho}{2} v^2 \tag{2.3}$$

$$v = \sqrt{\frac{2 D \Delta P}{f L \rho}} = \frac{4 Q}{\pi D^2} \tag{2.4}$$

to give a volumetric flow rate of:

$$Q = \sqrt{\frac{\pi^2 D^5 \, \Delta P}{8\, f\, L\, \rho}} \tag{2.5}$$

To obtain a solution the friction factor within each header and riser is required. In the laminar region (Re < 2300) the friction factor is calculated:

$$f = \frac{64}{Re} \tag{2.6}$$

where the Reynolds number (Re) is :

$$Re = \frac{VD}{\nu} \tag{2.7}$$

For turbulent flow (*Re* > 4000) the friction factor by Duffie and Beckman [4] is:

$$f = (0.79 \ln Re - 1.64)^{-2} \tag{2.8}$$

In the transition region from laminar to turbulent flow, which for smooth pipes is approximately:

$$2300 < Re < 4000 \tag{2.9}$$

The friction factor is calculated by linearizing between the two regions. A literature search revealed no discussion into this problem, indeed the true nature of the flow cannot be known due to the nature of the transition region. Two seemingly identical risers with the same flow rate could experience either laminar or turbulent flow due to a slight disturbance upstream in one of them which does not exist in the other. The NREL program was found to deal with this problem in the same way so is considered to be the best approximation to flow in this region.

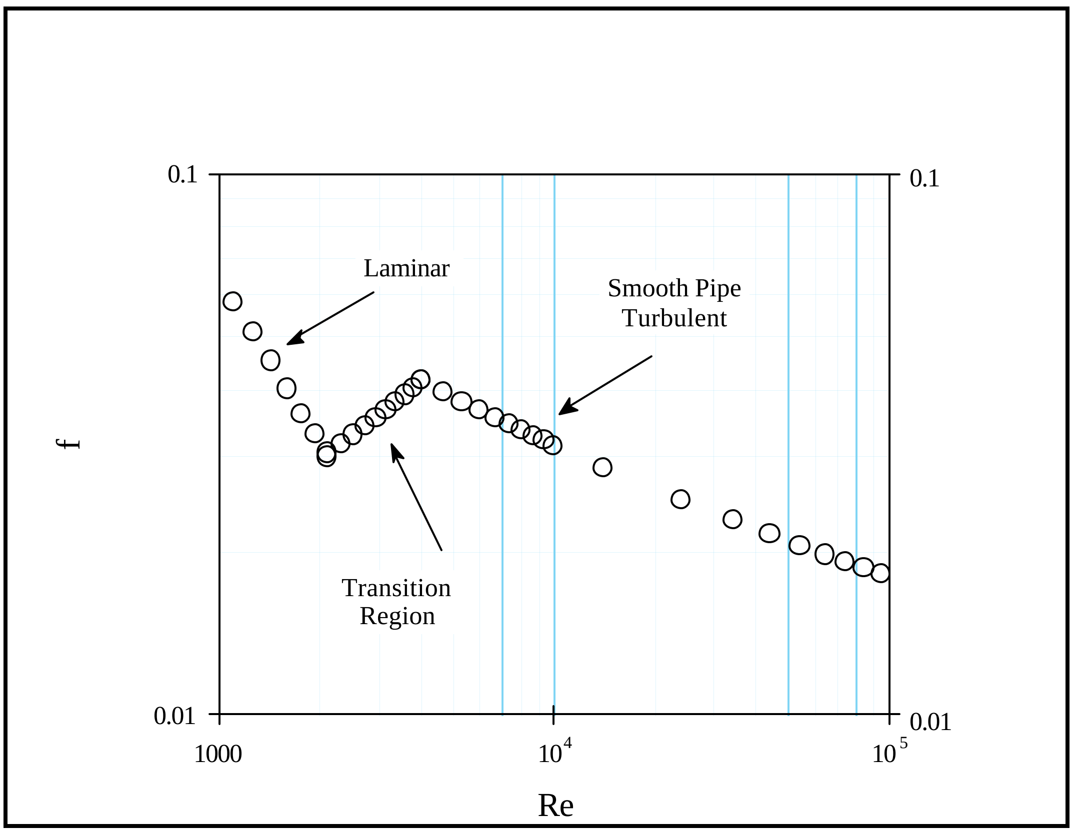


**Figure 2.3.2 Moody Diagram with Linearized Transition Region**

Beginning with an initial (arbitrary) inlet pressure at the lower header, the procedure is carried out by guessing the pressure drop in the first riser. With the pressure drop guessed, an iterative solution is required to obtain the flow rate in this riser (iterating with the friction factor and the flow rate). The flow through the riser is into the upper header which has a different diameter, Reynolds Number, and friction factor. With a known flow rate there is no need to iterate in the upper or lower headers. The pressure drop to the next riser is calculated in both lower and upper headers, so the pressure drop at the next riser is now known, and the iterative solution again yields the flow rate in this riser.

The procedure outlined is carried out in the entire set of risers until the last (See Figure 2.3.3). A correct solution is obtained when, at the last riser, the flow rate in the lower header is zero and the sum of the flows into the upper header is the total flow into the bank. When this situation is not satisfied the pressure drop guess in the first riser needs to be updated, i.e. re-run the program with a new guess.

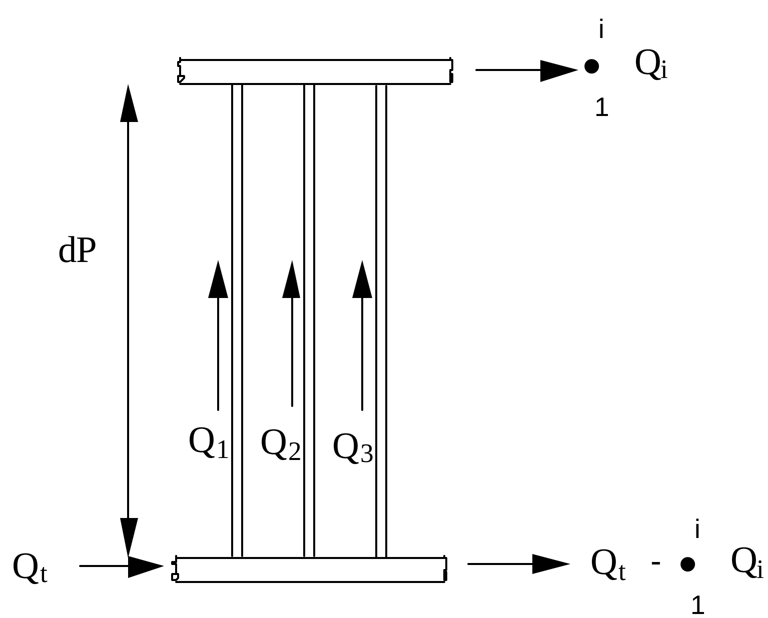


**Figure 2.3.3 Pipe Flow Analysis Program Schematic**

The flow rates yielded with the PFA method are available for each riser in the entire bank of collectors, but to simplify the presentation results and for easy comparison to NREL results, the average flow rate for each collector is calculated.

**NREL Solution**

A program to calculate the flow distribution in large banks of solar collectors connected in parallel was developed at NREL. Given flow drop characteristics of headers and collectors, an electrical circuit analogy is used such that V=I*R is analogous to dP=Q*R [13]. In other words the pressure drop is proportional to the flow rate in the collector-resistance-to-flow product.

The NREL program is menu driven and test condition information is input, such as the test flow rate, test fluid characteristics (density, specific heat, and the flow rate into the collector), and experimentally determined pressure drop. Next the user inputs the actual use conditions i.e., use fluid parameters, and total flow rate into the bank. Finally each header diameter, length and friction factor are input.

The pressure drop for the individual collector is a parameter which eliminates the need to input riser information. The number, length, and friction factor of each riser is never used. The pressure drop is an essential parameter to run the NREL program which accounts for all of the bends within each collector.

## 2.4 NREL vs. PFA RESULTS

The Pipe Flow and NREL solutions to the flow distribution problem were first tested using a simpler model of a collector which is easier to verify than such a complicated bank of collectors. Using pipe flow equations previously mentioned, for a 'test' flow rate of 2.5 GPM, and a single 48 inch long riser, the following equations were solved simultaneously for varying riser diameters using EES [15]:

| | |
|---|---|
| L=48 | (inch) |
| nu=0.739e-5 | ($ft^2/s$) |
| q=2.5 | (GPM) |
| rho=1.93 | ($slugs/ft^3$) |
| re=(4*q*12)/(pi*nu*d*7.481*60) | (ND) |
| f=(0.79*ln(re)-1.64)^(-2) | (ND) |
| v=(4*q*144)/(pi*d*d*7.481*60) | (ft/s) |
| dp=(f*L*rho*v*v)/(2*d*144) | (PSI) |

For riser diameters of 0.6 and 0.8 inch the pressure drop is 0.11401 and 0.02917 PSI, respectively. Five collectors were placed in parallel with this information and run in both the NREL and PFA programs. In both cases the flow was sufficiently poorly distributed to get a good comparison. A plot of the results for the diameter of 0.6 inch is presented below.

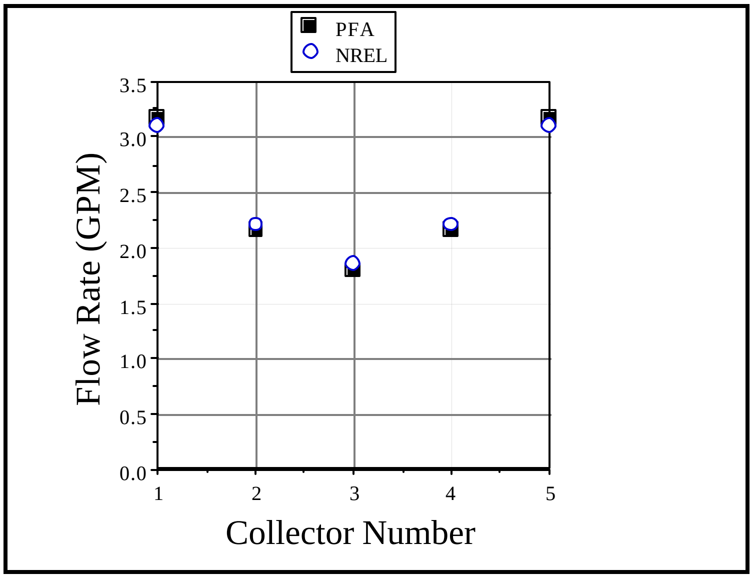


**Figure 2.4.1 NREL Vs PFA for Five Collectors**

With confidence that the two approaches are essentially the same, these two methods were then used for the bank of 15 collectors in parallel. They yielded very different results in the prediction of the distribution, and the approach needed to be re-evaluated. The flow distribution results without a bend loss coefficient are shown below.

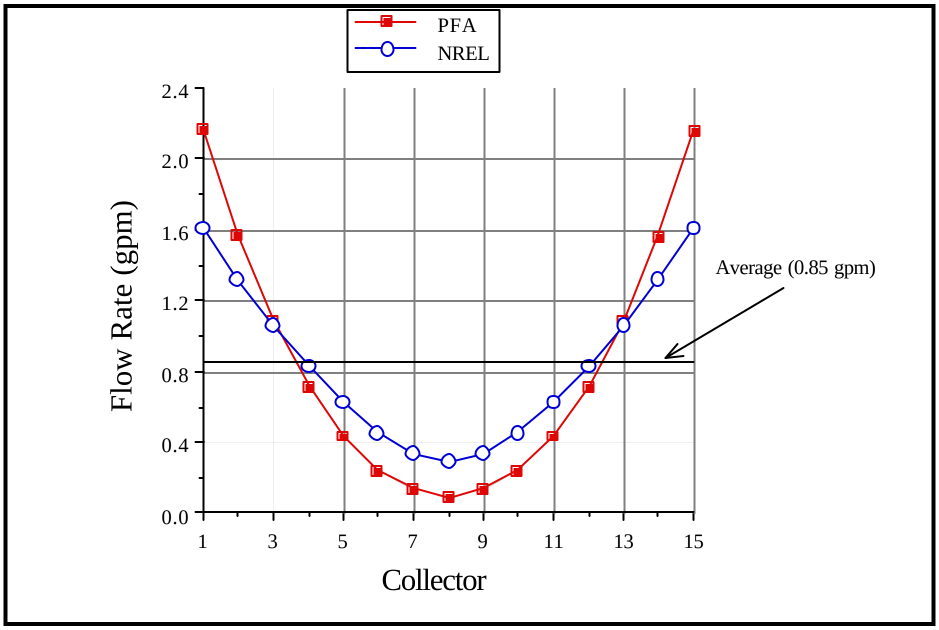


**Figure 2.4.2 Flow Distribution Without Bend Loss Coefficient**

For the five collectors in parallel of the test situation, the calculated pressure drop in the single riser collectors is due to only the length of the riser, and where headers and risers meet there is no pressure drop. So the two methods yielded nearly the same results for the flow distribution. In the actual collector with 17 risers, the measured pressure drop accounts for all the bends through which the fluid flows, and this needs to be accounted for in the Pipe Flow Analysis program. In other words, the theoretical collector has no pressure drop between headers and risers.

The energy equation has been re-written to account for the pressure drop between the headers and risers.

$$\frac{P_1}{\gamma} = \frac{P_2}{\gamma} + h_f + h_L \tag{2.10}$$

where $h_f$ is defined as:

$$h_f = f \frac{L}{D} \frac{v^2}{2\,g} \tag{2.11}$$

The units on Equation 2.10 are length. The previous solution had only the term $h_f$ but the head loss due to the bends can be added in with the term $h_L$.

$$h_L = K_e \frac{v^2}{2\,g} \tag{2.12}$$

The term $K_e$ is the bend coefficient which has been tabulated for a variety of area ratios and volumetric flow rates in the 1985 ASHRAE manual [7] for a Round Converging Tee.

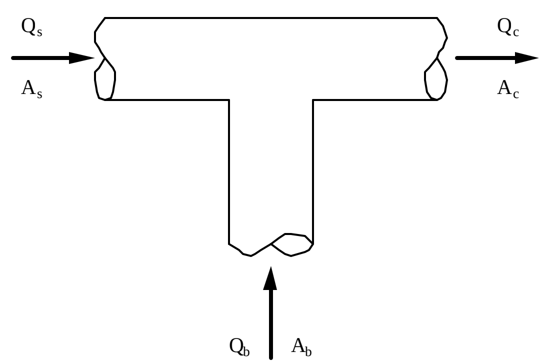


**Figure 2.4.3 Round Converging Tee**

The Packerland collectors have risers of 0.19 inch inner diameter and header inner diameters of one inch which is an area ratio of 0.036. The tabulated values in the ASHRAE manual are for area ratios no smaller than 0.1. It is probably not accurate to extrapolate $K_e$ values so far outside the range of reported values because the values for very small area ratios is quite non-linear at this point and gets extremely high as the area ratio goes to zero.

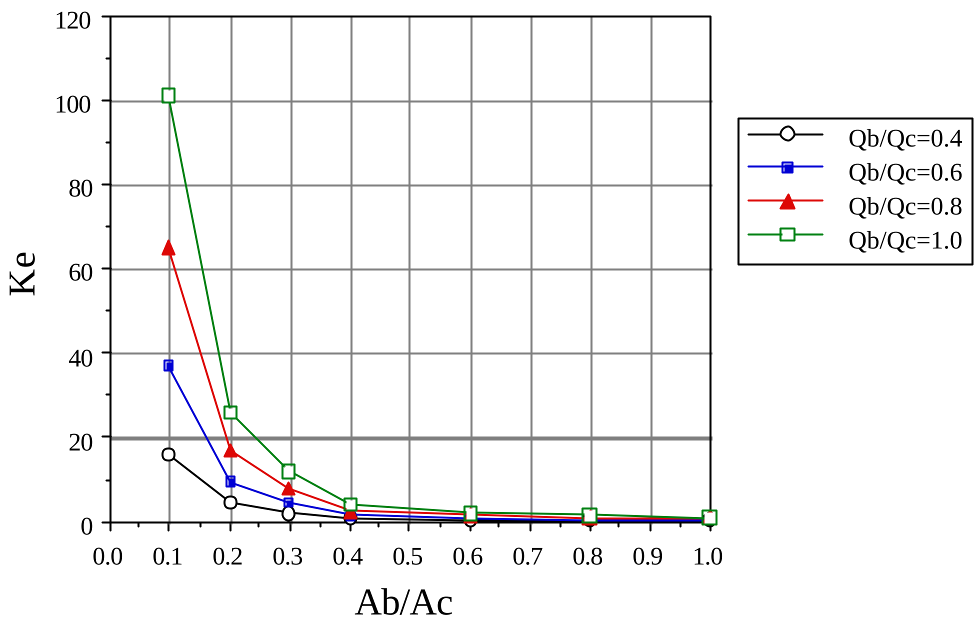


**Figure 2.4.4 ASHRAE $K_e$ Values for Round Converging Tee [7]**

Instead of attempting to extrapolate $K_e$ values out of the ASHRAE manual for varying volumetric flow rate ratios, a single value was assumed to apply for the entire collector bank of 15 collectors. The NREL solution to the flow distribution was generated and the $K_e$ value in the PFA solution was varied until the two solutions were nearly identical. The value of $K_e$ which yielded the correct solution for the PFA method was 37.5. It is a value which appears reasonable compared to the values provided in the ASHRAE manual (see Figure 2.4.4) on the low end of the area ratios in the table. The final flow distribution in a bank of 15 collectors is presented in Figure 2.4.5.

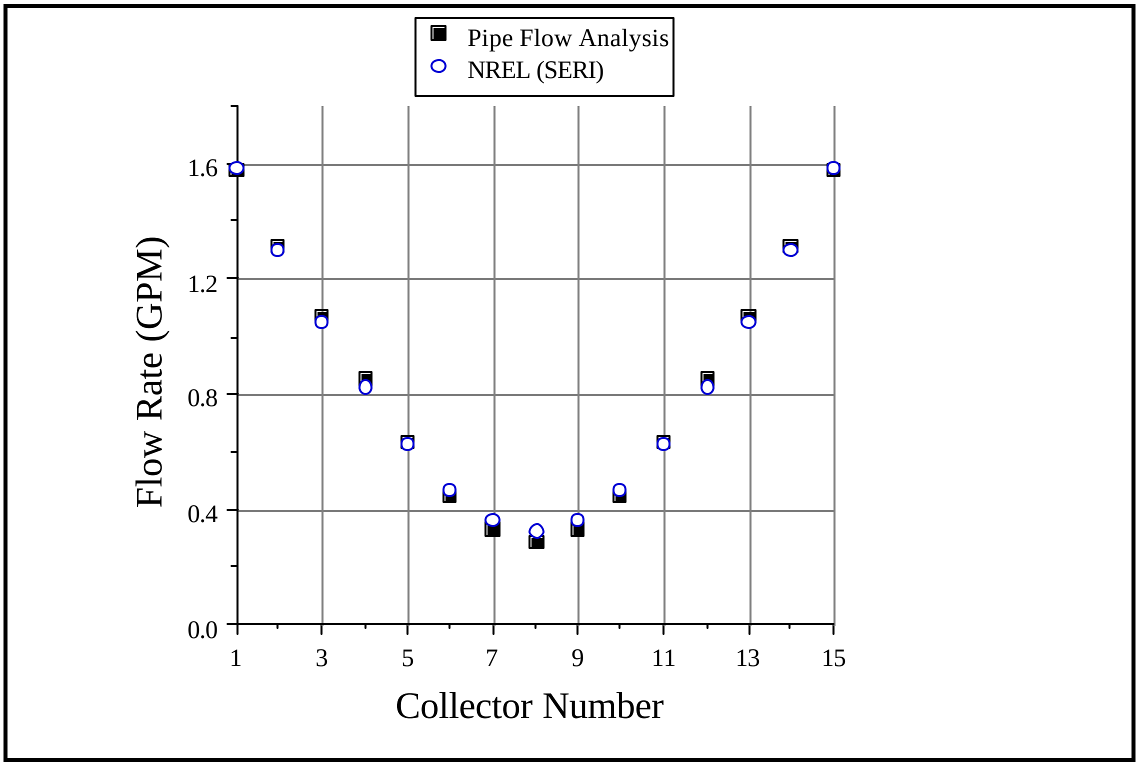


**Figure 2.4.5 Flow Distribution for 15 Collectors at Design Flow Rate**

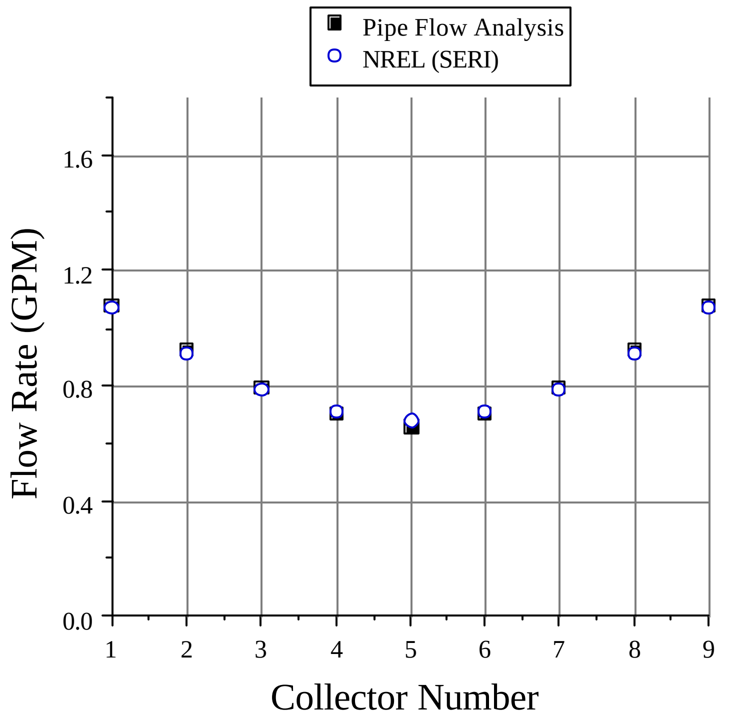


**Figure 2.4.6 Flow Distribution for 9 Collectors at Design Flow Rate**

Although the value for $K_e$ of 37.5 in the PFA method yields results which are quite similar to the NREL results, it remains to be seen if the same value would apply for different types of collectors. Clearly the advantage of this method, if found to be consistently accurate, is the ability to predict the flow distribution of large banks of collectors without first requiring the experimentally determined pressure drop. The PFA method requires only collector geometry, and although more difficult to apply than the NREL method, it would be possible to evaluate various collectors new on the market using the computer alone. Quite often manufacturers of flat plate collectors either don't provide or don't have pressure drop information on their collectors, so the NREL method would not be available for system designers.

## 2.5 NREL vs. PFA BANK PERFORMANCE RESULTS

Both the PFA and NREL methods were used to solve for the flow distribution of Packerland collectors in parallel banks of 9 and 15. Since the actual flow rate may be widely varied from bank to bank, a solution was obtained for a wide variety of flow rates. Each of the solutions for the flow rates were input to a table which was then solved with the following equation set (referring to Equation 2.1):

```
rho=61.17                                        {lbm/ft^3}
Qt=60*0.85/7.481                                 {ft^3/hr}
mdottest=rho*Qt                                  {lbm/hr}
Cpact=0.88                                       {btu/lbm-R}
Cptest=1.002                                     {Btu/lbm-R}
FrUl=0.89                                        {Btu/hr-R-ft^2}
Ac=31.5                                          {ft^2}
C1=mdottest*Cptest/Ac                            {Btu/hr-R-ft^2}
FprimeUl=-C1*ln(1-(FrUl/C1))                     {Btu/hr-R-ft^2}
Cact=(60/7.481)*Q*rho*Cpact/(FprimeUl*Ac)        {ND}
Ctest=C1/FprimeUl                                {ND}
Num=Cact*(1-exp(-1/Cact))                        {ND}
Denom=Ctest*(1-exp(-1/Ctest))                    {ND}
r=Num/Denom                                      {ND}
```

For a design flow rate of 0.85 GPM per collector, the Pipe Flow solution to the flow distribution of a bank of 15 (also Figure 2.4.5) was input to a table and solved. Figure 2.5.1 below contains the flow distribution data, and the corresponding collector performance. The average performance is 0.982 and the effective collector area is proportionally reduced by this value.

| Collector | Flow Rate (GPM) | Performance |
|---|---|---|
| 1 | 1.5747 | 1.013 |
| 2 | 1.3124 | 1.009 |
| 3 | 1.0703 | 1.003 |
| 4 | 0.8539 | 0.995 |
| 5 | 0.6384 | 0.982 |
| 6 | 0.4505 | 0.962 |
| 7 | 0.3319 | 0.937 |
| 8 | 0.2913 | 0.924 |
| 9 | 0.3319 | 0.937 |
| 10 | 0.4505 | 0.962 |
| 11 | 0.6384 | 0.982 |
| 12 | 0.8539 | 0.995 |
| 13 | 1.0703 | 1.003 |
| 14 | 1.3124 | 1.009 |
| 15 | 1.5747 | 1.013 |

**Figure 2.5.1 Design Conditions (Pipe Flow Analysis Solution)**

Applying Equations 2.1 and 2.2 to the flow distribution results of Section 2.4, Figure 2.5.1 shows the effects of the three factors which cause banks of collectors to operate differently than with the parameters obtained in the ASHRAE 93-77 [3], test for a variety of collector flow rates. The results of Figure 2.5.1 appear in Figure 2.5.2 as one point at an average flow rate of 0.85 GPM on the 15 collector curve.

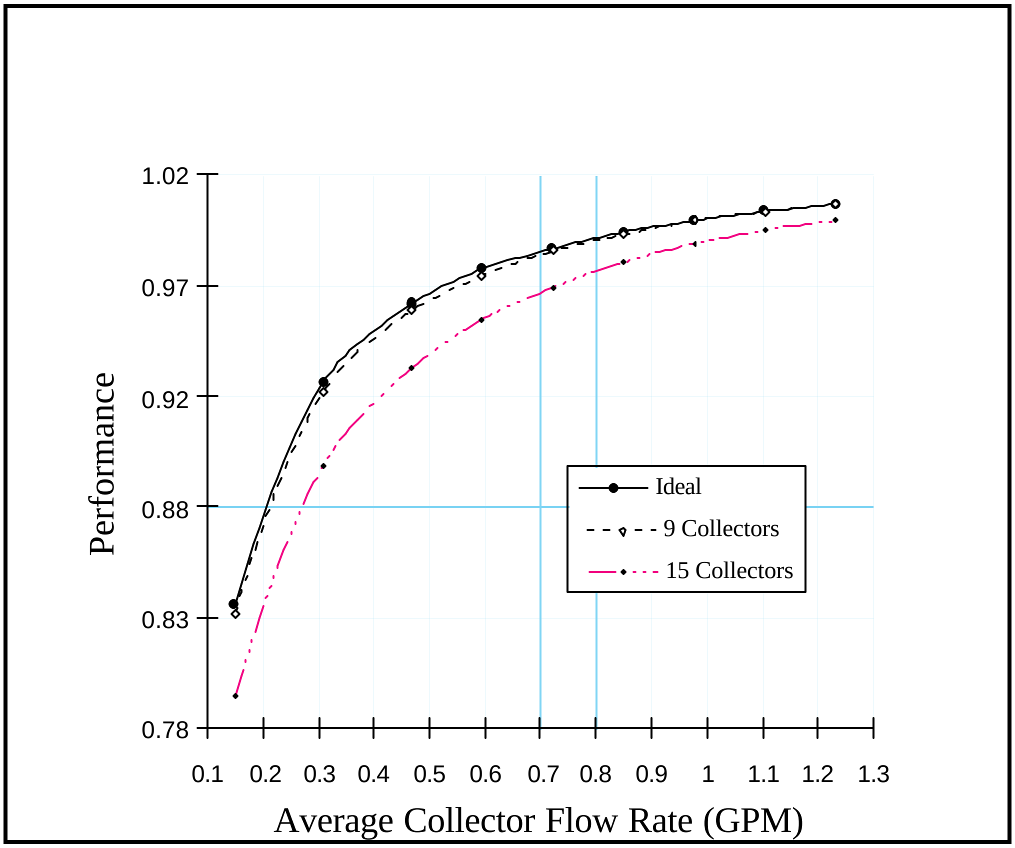


**Figure 2.5.2 Collector Bank Performance**

The three components which contribute to the performance curve are the effect of poor flow distribution within the collector bank, the working fluid specific heat, and the total mass flow rate. The ideal curve is that which would occur as a result of variable bank flow rate alone. The other two curves are a result of the flow distribution in the banks.

Clearly the effect of the collectors being connected in banks of 9 is negligible, relative to the ideal curve. The effect of the collectors being connected in banks of 15 is a matter of around two to four percent. The second component which contributes to the collector bank performance is the fluid specific heat. The collectors were tested using water which has a specific heat of 1.002 $\frac{\text{Btu}}{\text{lb}_m\text{°F}}$. The propylene glycol has a specific heat of approximately 0.88 $\frac{\text{Btu}}{\text{lb}_m\text{°F}}$. If the collector banks were operating with water, the ideal curve would be slightly higher, going through 1.0 at the design flow rate of 0.85 GPM. Thirdly, if the total bank flow rate were varied off of the design flow rate, the corresponding affect on performance can be seen in the graph.

CHAPTER
# THREE

## DATA ACQUISITION

The goal of this project is to successfully model the Packerland system with the intent of determining system efficiency and making recommendations which will improve the performance. It was to originally be accomplished by acquiring data on the system for a four to eight week period, but due to an unfortunate malfunction in the energy monitoring system two weeks after starting, recording had to be stopped.

### 3.1 RECORDING DEVICES

The data acquisition phase of the project was carried out by using three separate recording devices. The first device is what has been referred to so far as the Energy Monitoring Device. It operates 24 hours per day 365 days per year and calculates the energy output of the solar system provided to the meat packing plant (see Figure 1.2.1). It is located in the plant approximately 1400 feet from the storage tank. Over 15 minute intervals a **Badger** flow meter records the total mass flow rate and average temperature difference between the solar water and the city water. The number of therms provided in this period is calculated using Equation 3.1, recorded, and printed out on hard copy with a computing device manufactured by **Wahl**. Additionally, hourly totals and daily totals are tabulated. No other storage medium is used for this information.

$$\Delta Q = (m_{water}\, \Delta time)\ C_P\ \Delta T \tag{3.1}$$

The second device used was a computer connected to the outputs of two pyranometers. The output from a pyranometer is on the order of μV and the solar radiation measured is proportional to this amount by a constant determined when calibrated at the place of manufacture. The pyranometers used for this project were Model PSP manufactured by **The Eppley Laboratory, INC.** based in Newport, RI.

To ensure accuracy one of the pyranometers was returned to the manufacturer for re-calibration. An analog/digital board was purchased from **OMEGA** for the recording of data on an IBM computer. The calibrated pyranometer was run next to the uncalibrated pyranometer on a sunny day, and the calibration constant for the second pyranometer was then determined. At Packerland the pyranometers were set up out on the array, one on the tilt of the bank and the other on the horizontal as shown.

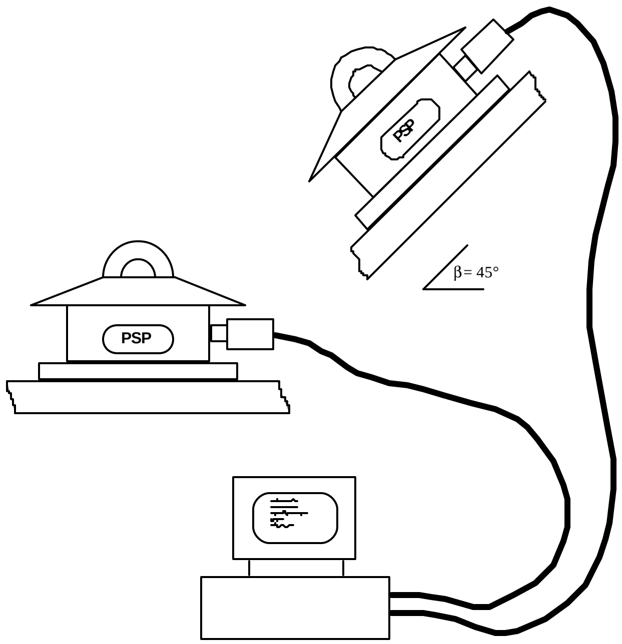


**Figure 3.1.1 Solar Radiation Recording With Eppley Pyranometers**

The third recording device was a different IBM computer provided by Packerland Solar Systems. On it were recorded a series of temperatures used for control and other purposes located throughout the system, and the tank level (Figure 3.1.2). The temperature sensors are called **Resistance Temperature Dependent** (RTD) sensors. They are a platinum resistor which varies resistance as a function of temperature. The RTD's are normally used for control purposes and monitoring tank temperatures, etc.., so it was only a matter of tapping into the existing hardware and recording values.

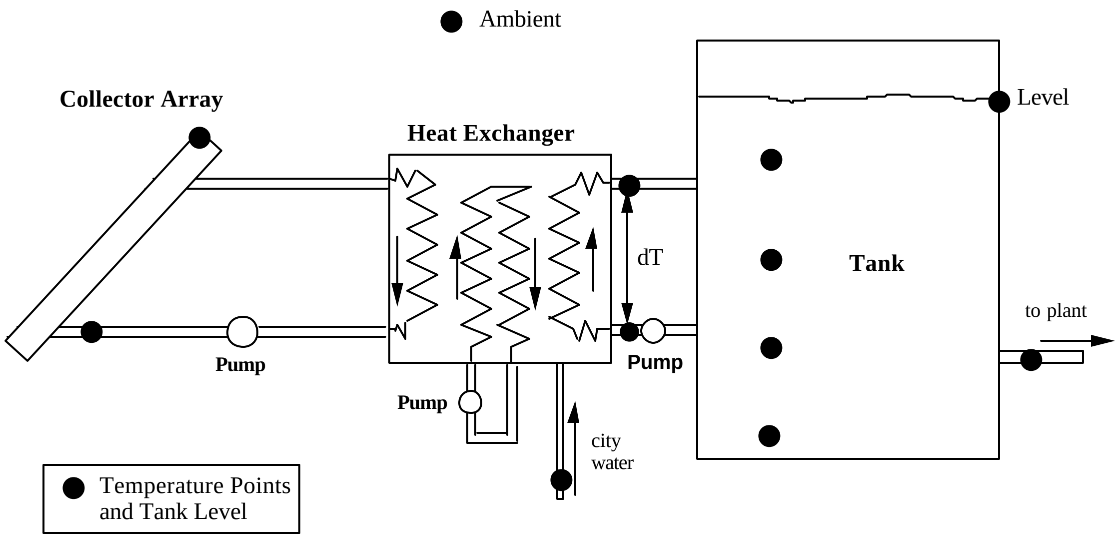


**Figure 3.1.2 Plant Temperatures and Tank Level**

Eleven values were recorded throughout the plant as indicated in the diagram. Four tank temperatures at 2,9,17, and 25 feet from the bottom. The temperature to the plant, city water, collector array, array return temperatures and the temperature across the heat exchanger on the water side, which is a measure used for control purposes were recorded. The tank level was also recorded.

## 3.2 DATA LOGGING AND FILE PREPARATION

The two IBM computers were set to monitor data at two minute intervals. Beginning on July 19, 1991 at 2:45 PM data logging was begun, and went uninterrupted for two weeks. Unfortunately the **Wahl** energy monitor broke down and monitoring had to be stopped because without load information other plant information would not be useful.

There was another unfortunate occurrence after data acquisition was discontinued. While the load data for the two week period was waiting to be copied it was misplaced up at the plant in Green Bay, so the 15 minute energy data were not available for modeling purposes. Fortunately the 24 hour totals of both water drawn and energy provided were recorded and available for the project.

A total of five gaps in the data occurred during the two week period during file saving and computer start-up. In each case it occurred during the morning hours when the solar radiation was still low and not much was happening with the system. Three of the gaps were approximately 6 minutes with a clear trend in the solar radiation which was interpolated into the file. The other two gaps were less than 30 minutes and the approximate trend in the solar radiation was added to the file for this time. Again, since the level of radiation was low, and the time period was relatively short, the affect of this approximation is considered negligible. The approximation was done because to model with TRNSYS for the entire two week period, a continuous solar radiation and temperature file are required for the whole period.

The two IBM computers used for the project had different clock speeds so a time correction was calculated for each and applied to the files.

The temperature files were combined into one large file at two minute intervals. A program was written to take average temperatures and tank level over a 15 minute period and these values were written into a new file. The file starts at 4790.875 hours, and ends at 5121.375. During the same time period the solar radiation for both tilt and horizontal were put onto a different file over 15 minute intervals. The original two minute data was integrated over the 15 minute period and the average was taken. Into these files were put the approximations for the gap information previously discussed.

For the 11 day model of the system, the files were reduced from their original length of almost 15 days. The files were produced from the two minute interval data. Rad.dat contains four columns; time (hr), horizontal radiation (Btu/ft^2-hr), tilt radiation (Btu/ft^2-hr), and the number of original data points in two minute intervals which went into the 15 minute interval. The last column can be used to determine where the five time gaps in the data acquisition occurred. Normally this value is seven or eight.

The other file produced for the 11 day model is TWA2.dat (Time, Water, Ambient data). The water and ambient temperatures were averaged over each 15 minute period and placed in this file. These two files have been provided on disk with the master copy of this thesis to the UW-Madison Solar Energy Laboratory and can be obtained upon request. An example of the data is provided in the Appendix.

CHAPTER
# FOUR

## SYSTEM MODELING

The Packerland energy output has been modeled with both *f*-Chart [8] and TRNSYS [1]. The *f*-Chart method is quite easy to apply and evaluate. The TRNSYS system, on the other hand, requires more detailed estimates of the loss coefficients and mass flow rates but should yield more accurate results. Chapter Four discusses these system parameters, then goes on to cover results of both the eleven day TRNSYS simulations and the annual runs and shows how they compare to the actual system output. Lastly the current control strategy employed by Packerland Solar Systems is evaluated.

### 4.1 *f*-CHART ANALYSIS

*f*-Chart [8] is a computer program developed for designers of solar domestic hot water systems as a means of determining and meeting a certain load requirement with a solar system. Empirical correlations developed by Klein [16] have been incorporated into the *f*-Chart program. The parameters for the Packerland system were input to *f*-Chart as a means of determining an approximation of the energy output for the Packerland system. The purpose of performing the *f*-Chart calculations is to determine to what extent the results apply to a system of this size.

The energy output of the Packerland system is available from the year the system was re-built in 1987 to 1991. However for 1987 and 1988 the system was not fully operational so the *f*-Chart analysis is not performed for these years.

Data available on the output of the system are reported in therms and gallons of water provided for the year. The 'Days of Operation' is the number of days in the year during which water was drawn by the meat packing plant, *not* the number of days the system actually operated. The 'Number of Panel Days' is the total number of panels which were operating during the year for the total days of operation.

| | 1987 | 1988 | 1989 | 1990 | 1991 |
|---|---|---|---|---|---|
| Therms[1] | 103.1 | 198.5 | 257.3 | 260.6 | 308.0 |
| Gallons[2] Water | 38.60 | 56.26 | 54.67 | 68.08 | 93.29 |
| Days of Operation | 179 | 245 | 251 | 224 | 257 |
| Panel[3] Days | 0.3526 | 0.6541 | 1.294 | 1.115 | 1.333 |

1. Therms reported in thousands
2. Gallons water reported in millions
3. Panel days reported in millions

**Figure 4.1.1 Packerland Output**

The average daily load for the year is required in the *f*-Chart calculations. No load profile can be input to *f*-Chart. The Packerland load generally occurs only during the week, and although there is no draw on the weekend, the system still collects solar energy. The average daily load flow was then taken to be the total number of gallons drawn for the year divided by the number of days in a year.

The number of collector panels input to the *f*-Chart solutions are the number of panel days divided by the days of operation. Although not the actual number of collector panels which were in operation for the year, it is an approximation which is an *effective* number of panels for the year. The actual collector flow rate/area input is 0.238 GPM/collector, or 3.908 $\frac{lb_m}{hr\text{-}ft^2}$, the derivation of which will be shown later in the section on the glycol flow rate (Section 4.3).

The Water Storage System in the *f*-Chart program was used to evaluate the Packerland System. The energy provided for each year can be calculated from the output table of *f*-Chart.

$$E_{system} = Load * f \qquad (4.1)$$

The load is determined from the water set point in the program which was 150°F for all annual calculations. The energy provided by the system is the load flow for the year at a temperature of 150°F which is heated from the mains water temperature.

The $f$-Chart program allows the user to input either the number of collector glazings or a constant incidence angle modifier. A single glazing and a constant incidence angle modifier of 0.23 were run in the $f$-Chart program for 1989, 90, and 91, the results of which are shown in Figure 4.1.3. No tank or pipe losses were considered in the $f$-Chart calculations as a means to establish an upper limit for energy output under the current system hardware.

The data for 1990 were input to the $f$-Chart program:

A summary of *f*-Chart results is shown which were derived using the above assumptions.

| Year | Daily Load Flow ($lb_m$/day) | Number of Collector Panels | Actual Energy (Therms[1]) |
|---|---|---|---|
| 1989 | 1249000 | 5156 | 257.3 |
| 1990 | 1556000 | 4978 | 260.6 |
| 1991 | 2132000 | 5187 | 308.0 |

1. Therms reported in thousands

**Figure 4.1.2 Actual System Operation**

| Year | Annual Load (Therms[1]) | Single Glazing Load Fraction | $b_0$ = 0.23 Load Fraction | Single Glazing Energy (Therms[1]) | $b_0$ = 0.23 Energy (Therms[1]) |
|---|---|---|---|---|---|
| 1989 | 483890 | 0.520 | 0.467 | 252 | 226 |
| 1990 | 602440 | 0.433 | 0.386 | 261 | 233 |
| 1991 | 825660 | 0.346 | 0.307 | 286 | 253 |

1. Therms reported in thousands

**Figure 4.1.3 *f*-Chart Output**

The *f*-Chart method is a somewhat simplified model compared to the TRNSYS model. For instance, *f*-Chart can not account for the benefits of a highly stratified storage tank. The *f*-Chart method uses average solar data, as does the annual TRNSYS model using the weather generator, so energy output cannot be directly compared to the actual output. The *f*-Chart method calculates the energy output within 5 percent for the single glazing collector. The calculations based on the constant incidence angle modifier were consistently around 10 percent lower than the single glazing system output.

An eleven day TRNSYS model of the Packerland system has been developed using solar radiation measured parallel to the collector surface. The results of the TRNSYS simulations will be presented in Sections 4.4 and 4.5 with a comparison to the *f*-Chart results just presented.

## 4.2 TRNSYS MODEL

This section is devoted to describing the TRNSYS system and the parameters of the components used. The following section describes the load for the eleven day model and the derivation of the various parameters specifically applied to the Packerland System.

A TRNSYS model was developed to determine and verify system parameters using the data acquired on the system during the two weeks in the summer of 1991. The load profile was constructed using the tank level and total draw from the tank for each day . For the first weekend, since data acquisition started on Friday, the energy reported on that day is difficult to separate out from what was actually drawn on the weekend. The simulation time is then an eleven day period starting at hour 4848 (Monday, July 22, 1991 12:00 AM) and going to hour 5112 (Thursday, August 1, 12:00 PM). For the same reason the last day of the simulation is a Thursday since the reported Friday energy total also includes that of the following weekend.

Figure 4.2.1 represents all major components and was used to write the information flow diagram (Figure 4.2.2) for the system. The main simplifications which differ from the actual system are for the pump 1 and 2 controllers, and the entrance of the supply water for the model to the tank.

Pump 1 controller turns on the glycol loop when sufficient solar radiation is present to obtain useful energy. In the real system this is very nearly the case except that only one pump is used during the warm up of the glycol, after which time all four pumps are turned on and remain so for the rest of the day. Pump 2 controller turns on when the temperature of the glycol out of the pipe (Unit 12 Type 31) exceeds the tank bottom temperature by 1°F. The actual control of these pumps is a complicated process which increases the number of pumps on the tank side and on the inner loop of the heat exchanger. Instead of increasing the pumps as in the real system, a single mass flow rate between tank and heat exchanger occurs when the number 2 controller turns on. The eleven day TRNSYS model results (Section 4.4) will include energy output for variation of this mass flow rate (more realistically) to indicate that this selection of constant mass flow rate for the entire period sufficiently represents the system.

The city water is pumped directly into the cold side of the heat exchanger (see Figure 1.2.3). The TRNSYS model is somewhat simplified in that the supply water goes to the tank bottom instead. The one node tank model, since complete mixing occurs in the tank, is not expected to accurately represent the system. However for the two and multi-node tank models, since the heat exchanger draw is from the cold tank bottom, the system is fairly accurately represented. Recommendations based on the TRNSYS results are predicted for the system which achieves a certain level of stratification and will be based on these results.

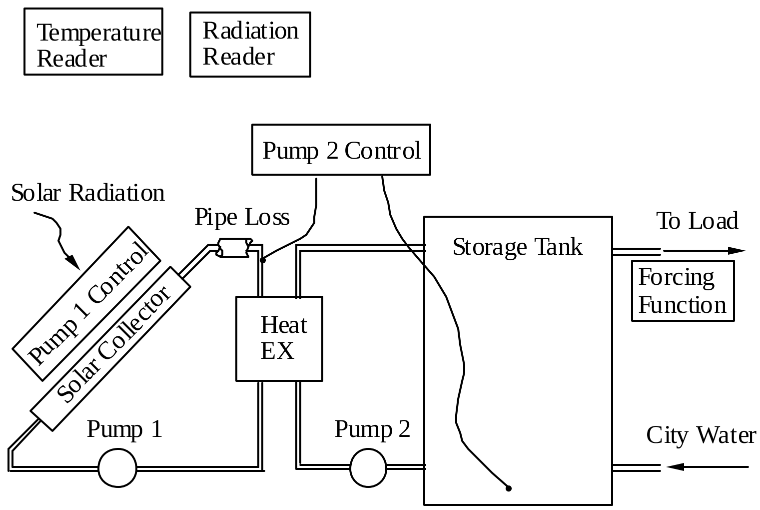


**Figure 4.2.1 TRNSYS System**

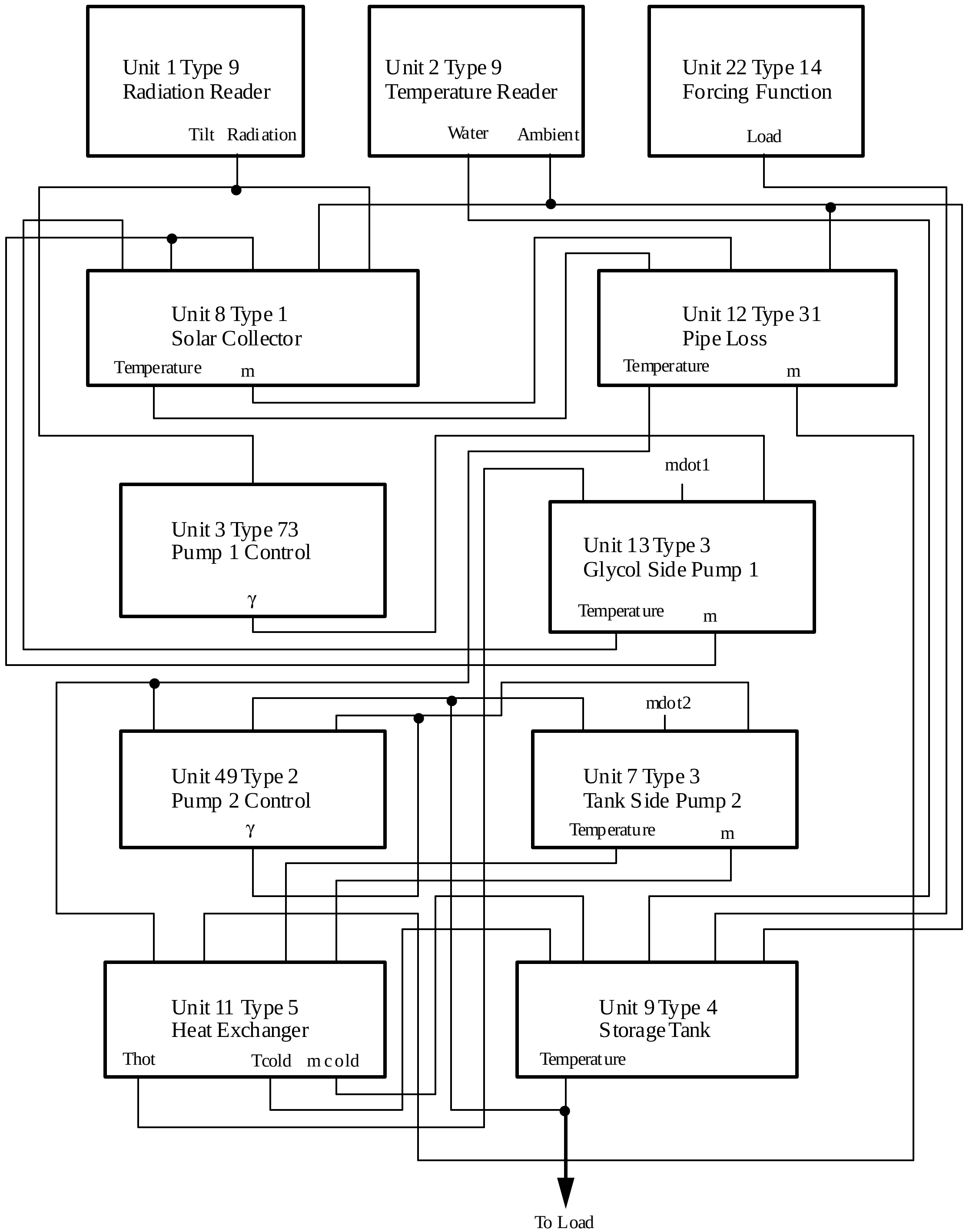


**Figure 4.2.2 Information Flow Diagram**

Only the first five solar collector inputs are used for the model because the solar radiation files are taken on the tilt, and the radiation processor is not used. All other inputs and parameters are standard for flat plate solar collectors as described in the TRNSYS manual.

The storage tank model enables the user to input a different number of nodes for different runs to account for temperature stratification within the tank. A one node model calculates system output for a completely mixed tank. The tank loss coefficient is based on exposed surface area.

## 4.3 LOAD AND SYSTEM PARAMETERS

**Glycol Loop Control**

The control of the overall system is semi-automatic in nature. The glycol pumps are turned on when there is sufficient solar radiation to collect useful energy with the system. It is described as semi-automatic because the operator quite often overrides the controller and runs the system manually. As an example; when the mains water warms overnight (in the underground piping) from its supply temperature of say 36°F to a ground temperature of 55°F, the system is turned on because the operator knows (from the previous days operation) the supply water is truly below what the temperature sensors are reading. When to turn on the pumps is determined by the operator, based on his several years of experience at Packerland. Although this somewhat subjective control may introduce slight variations in the control strategy, it usually occurs during times of low solar radiation so its effect on system performance is small.

There are approximately 27000 gallons of glycol in the total collector and heat exchanger piping [12]. Some of the collected energy during each startup of operation goes to warming the glycol before there can be any useful energy output. It will be assumed that useful energy can be collected from the system when the glycol is warmed above the supply water temperature (see Section 4.6). The energy required to warm the glycol can be calculated based on actual glycol/mains water temperatures for the eleven day simulation. However, for the annual simulations this analysis does not have the benefit of yearly measured glycol and water temperatures so some approximations are needed.

An energy balance was performed on the glycol to estimate the solar radiation required to warm the glycol above supply water temperature. From the data file taken during the two week period on the system at Packerland, glycol and supply water temperatures were used (at 6:00 AM, just before sunrise) on the eleven days during which the TRNSYS simulation occurred.

| Time (hr) | Tglycol (°F) | Tsupply (°F) | ΔT (°F) | ΔE (Therms) |
|---|---|---|---|---|
| 4854 | 70 | 50 | negative | NA |
| 4878 | 59 | 50 | negative | NA |
| 4902 | 57 | 53 | negative | NA |
| 4926 | 51 | 56 | 5 | 10.2 |
| 4950 | 49 | 60 | 11 | 22.5 |
| 4974 | 47 | 62 | 15 | 30.7 |
| 4998 | 63 | 68 | 5 | 10.2 |
| 5022 | 60 | 68 | 8 | 16.4 |
| 5046 | 53 | 69 | 16 | 32.8 |
| 5070 | 62 | 69 | 7 | 14.3 |
| 5094 | 55 | 64 | 9 | 18.4 |

**Figure 4.3.1 Energy Required to Obtain Useful Energy From the System**

Over the eleven day period the average amount of energy required to heat the glycol to provide useful energy is 14 therms.

Using solar insolation data from July 23 and 24 (these were two sunny days), the useful energy equation [4] was written for the morning data.

$$Q_u=A_c[F_R(\tau\alpha)I_T-F_RU_L(T_i-T_a)] \qquad (4.2)$$

The ambient temperature in all cases was above the glycol temperature so the losses in the equation will be neglected.

$$Q_u=A_cF_R(\tau\alpha)I_T \qquad (4.3)$$

Equation 4.3 is really an energy rate equation which must be integrated over time, or taken over time increments with the following:

$$Q_u=\sum_{i=1}^{N} A_cF_R(\tau\alpha)I_T\Delta t \qquad (4.4)$$

The solar data are in 15 minute intervals. The sum of the useful energy was calculated using the solar data on these two days. Shown below are the results for both days. It was determined the glycol would be sufficiently warm (on the average) when the solar radiation has input 14 therms of energy input, which although will vary from day to day, occurs at a level of radiation of approximately 16 Btu/hr. This has been chosen as the control parameter for the glycol loop in the summer months. When the solar radiation is above Imin equal to 16 Btu/hr, the glycol pumps turn on and the system collects useful energy. For the eleven day TRNSYS simulation of the system this parameter will be varied to 5, 30, and 45 Btu/hr as a means of demonstrating the energy output from the system is not highly dependent on the selection of this parameter. These results will be presented in Section 4.4.

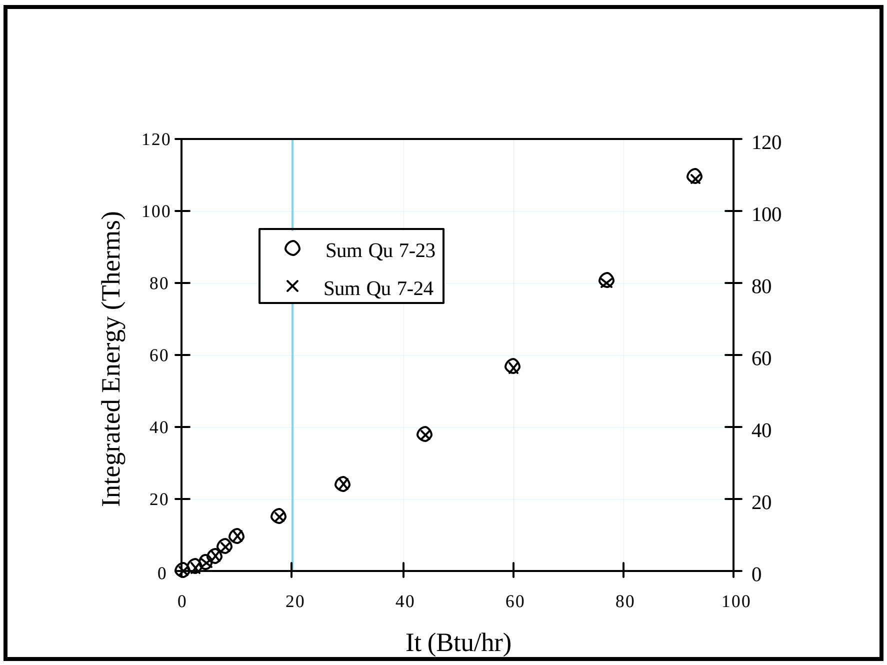


**Figure 4.3.2 Sum Qu for Imin Determination**

The same approach is taken for the annual simulations . Assuming morning glycol temperatures of -10 °F for the months of December-February, 25 °F for the months of March-May and Sep-Nov, and a supply water temperature of 45 °F throughout the year, the amount of energy to heat the glycol to a useful temperature is calculated. These morning glycol temperatures were chosen, perhaps on the cold side, as a means of estimating the required energy input to the glycol which will err to the conservative side. The mains supply water temperature of 45°F was chosen higher than average for the same reason. Imin of 16 Btu/hr will be used for the months of June-August as found in the previous analysis.

The amount of energy to warm the glycol is 112 therms for a temperature increase of 55°F in winter, which occurs at about 95 Btu/hr. The spring and fall temperature increases of 20°F requires 41 therms which occurs at about 47 Btu/hr. These are the parameters used in the annual TRNSYS simulations to determine when to turn on pump 1.

**Glycol Flow Rate**

Two methods were used to determine the flow rate of the glycol in the collector loop. The first was by performing an energy balance on the heat exchanger. The water pumps between the tank and heat exchanger were turned off and the city water valve was opened up. Since there is a flow meter on the city water line, the flow rate into the cold side of the heat exchanger was known. The inner water loop to the heat exchanger can be neglected since an energy balance will yield the glycol mass flow rate regardless of what occurs in the heat exchanger.

With all four pumps on the glycol side on, the four temperatures into and out of the heat exchanger were recorded after all temperatures had stabilized. For a water side mass flow rate of 740 GPM, the cold side temperatures in and out of the heat exchanger were 38 and 74 °F, respectively. Correspondingly the hot side temperatures in and out were 90 and 67 °F. The effectiveness of the heat exchanger can be calculated using simply the ratio of two temperature differences if the minimum fluid capacitance is known. From Incropera and De Witt [11]:

$$\varepsilon=\frac{C_c(T_{c,o}-T_{c,i})}{C_{min}(T_{h,i}-T_{c,i})} \tag{4.5}$$

The minimum capacitance for these conditions is on the water side (the cold side) so the thermal capacitances cancel and the effectiveness is 0.69.

Performing an energy balance on the heat exchanger, and assuming all flows and temperatures have reached steady state, the flow rate on the glycol side is determined by:

$$m_{water}C_{p,water}(T_{co}-T_{ci}) = m_{glycol}\,C_{p,glycol}\,(T_{hi}-T_{ho}) \tag{4.6}$$

substituting density and volumetric flow rate for mass flow rate:

$$\rho_{water}Q_{water}C_{p,water}(T_{co}-T_{ci}) = \rho_{glycol}Q_{glycol}C_{p,glycol}\,(T_{hi}-T_{ho}) \tag{4.7}$$

Solving for the glycol volumetric flow rate yields approximately 1250 GPM. The total system contains 5256 collectors which results in a flow rate of 0.238 GPM/collector. In the *f*-Chart program, the glycol flow rate per area is required in units of $\frac{lb_m}{hr\text{-}ft^2}$. 0.238 GPM/collector converts to 3.908 $\frac{lb_m}{hr\text{-}ft^2}$ using 31.5 $ft^2$ gross area.

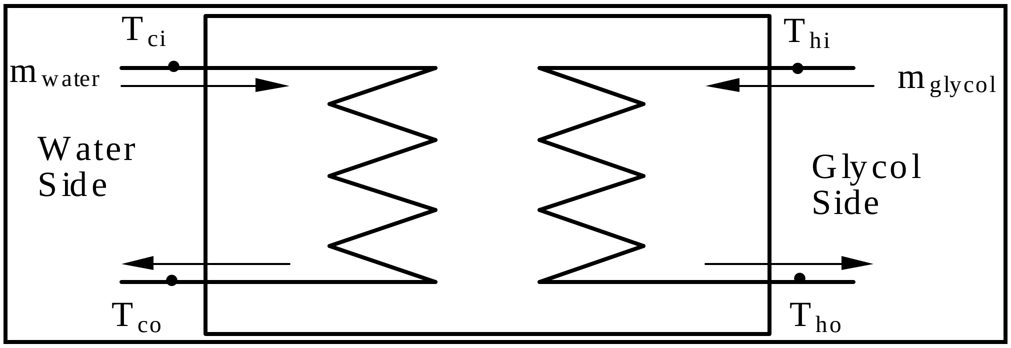


**Figure 4.3.3 Heat Exchanger Energy Balance**

The second means of determining the glycol flow rate was with an ultrasonic flow meter manufactured by **Polysonics Hydra**, located in Houston, Texas. This is a non-invasive flow meter utilizing the Doppler Effect as the basic principal of operation. A twin transducer is mounted on the exterior of the pipe so there is no physical contact between the transducer and the liquid. One of the crystals transmits a continuous ultrasonic wave through the pipe wall and into the fluid stream. A small portion of the energy is reflected back to the receiver as a Doppler shifted frequency [17].

The flow meter was first tried on the city water line on which there is also a mechanical flow meter which had been replaced one week prior to these readings. The water line is the only one in the plant which has a flow meter against which the ultrasonic readings could be compared. Due to its recent calibration the mechanical meter is considered the more accurate of the two. Also, the ultrasonic meter operates best with a dirty or bubbly liquid, so any results which vary from the mechanical meter are immediately put into question since this is potable city water being measured.

Two separate readings on the water pipe were taken when the mechanical meter read 675, then 831 GPM. Shown below are the results of the comparison of the ultrasonic to the mechanical meter. The percent error is based on the mechanical meter readings.

| Reading Number | Mechanical Flowmeter (GPM) | Ultrasonic Flowmeter (GPM) | Percent Error |
|---|---|---|---|
| 1 | 831 | 600 | -27.8 |
| 2 | 831 | 636 | -23.4 |
| 3 | 675 | 441 | -34.7 |
| 4 | 675 | 453 | -32.9 |

**Figure 4.3.4 Ultrasonic Vs Mechanical Flow meter Water Readings**

Since the accuracy of the ultrasonic flow meter could not be verified to anything better than -23.4 percent, the results from the glycol readings could only be expected to yield results in the vicinity of the actual flow rate. The four glycol pumps were turned on and four readings were taken. The four glycol flow rates were 537, 807, 777, and 688 GPM. These flow rates are fairly consistent with the results of the energy balance and the measure of the water flow rate. The values are between 35 and 57 percent below the value obtained by the energy balance.

A value of 1250 GPM is used as the propylene glycol volumetric flow rate. Some effort will later be made into determining how sensitive the results of this study are to the selection and use of this value, and this will be discussed in Section 4.4.

**Tank Side Water Flow Rate**

There are three pumps between the tank and the heat exchanger which operate under a complicated control strategy which is designed to extract the maximum energy from the glycol. The basic control assumption is that for full operation of the system (i.e. high solar radiation), the maximum energy can be extracted from the glycol with the maximum flow rate on the water side of the heat exchanger. During early morning hours one pump is turned on for low levels of radiation. The number of pumps turned on increases as the level of solar radiation increases. Near the end of the day the number of pumps is reduced in much the same way.

The TRNSYS model was simplified from this control strategy in that when the pumps are turned on, one total mass flow rate results from all three. In other words the ability to increase the mass flow rate on the water side of the heat exchanger with one, two or three pumps was not built into the model. This simplification was made because on the days of high solar radiation, all three pumps come on quickly in the morning and stay on all day. For most of the solar collection throughout the summer (which makes up much of the annual solar collection) this is the case, and the majority of the energy gathered by the system occurs with three pumps on. The eleven day TRNSYS model was run with this flow rate varied throughout the day to demonstrate the results are not highly dependent on this parameter when operating as the current system does. These results will be presented in Section 4.4.

The tank side water flow rate with all three pumps on and the supply water valve wide open was determined by applying an energy balance to the two converging flow streams before and after they mix. The city water mixes with the tank water before entering the heat exchanger on the cold side. By measuring the supply water flow rate, its temperature, the tank water pre-mix temperature, and the mix temperature it is possible to back out the flow rate of the pre-mix water. The energy balance yields the following equation, assuming constant specific heat and density.

$$Q_{tank} = Q_{supply} \frac{(T_{supply} - T_{mix})}{(T_{mix} - T_{tank})} \tag{4.8}$$

For all three pumps on, the supply water was measured to be 35.6°F with a volumetric flow rate of 660 GPM. The mix temperature was 77.0°F, and the tank was at 84.2°F (see Figure 4.3.5). This results in a supply flow rate from the three pumps alone to be 3795 GPM. The total volumetric flow rate of the water into the heat exchanger is 4460 GPM or approximately 4500. This is the value assumed to be the operating flow rate for the TRNSYS model. The same method was applied to obtain flow rates between the tank and heat exchanger for one and two pumps as well. With one pump the mass flow rate is 2770 GPM and for two pumps it is 3420 GPM.

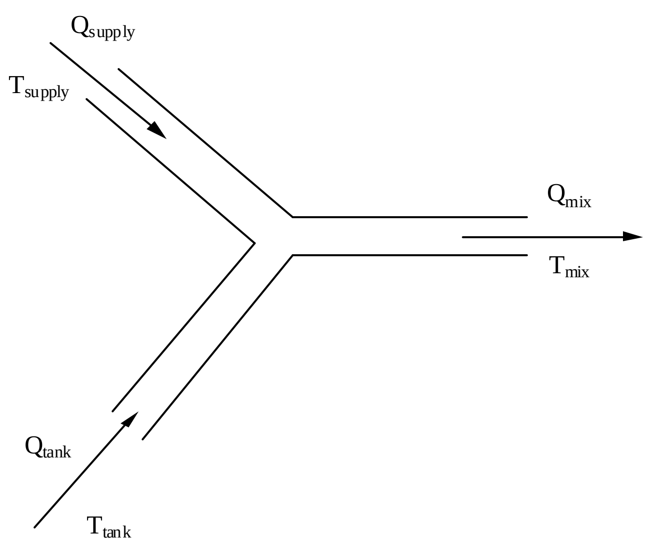


**Figure 4.3.5 Tank Side Mass Flow Rate Determination**

**Pipe Loss Coefficient**

The Packerland system has roughly 8000 to 9000 feet of 8 inch pipe between the feed and return lines in the glycol loop. Additionally there are about 4000 feet of 1 inch couplings (uninsulated copper), 1600 feet of 1 inch flex tubing (rubber insulated), and about 350 feet of 3 inch flex tubing (uninsulated). The 8 inch pipe has two to three inch insulation over most of its length, but has some sections where the insulation has been removed or has deteriorated.

The task of determining the pipe loss coefficient for the overall system has been simplified by assuming 5000 feet (half of the total comes in hot from the array) of 8 inch pipe between the outlet of the collector array and the inlet to the heat exchanger. The operator of the system states that based on his experience there is on the order of about a one to three degree temperature drop between the collector outlet and the heat exchanger inlet [12].

An energy balance was written on this 5000 foot length of pipe, and the pipe loss coefficient was calculated for two temperature drops of the glycol (1°F and 2.5°F) as a means of estimating an upper and lower bound of the system pipe loss coefficient. Based on a set of both the glycol and ambient temperatures taken during the two week data acquisition period, these lower and upper pipe loss coefficients were calculated with the following and are presented in the table below.

$$u_p = \frac{mC_p(T_{c,out} - T_{hx,in})}{\pi D_p L_p(\overline{T}_p - \overline{T}_a)} \qquad (4.9)$$

| Time (hour) | $\overline{T}_p$ | $\overline{T}_a$ | $u_{p,low}$[1] | $u_{p,high}$[1] |
|---|---|---|---|---|
| 4791 | 141 | 91 | 1.086 | 2.715 |
| 4864 | 135 | 90 | 1.2083 | 3.021 |
| 4884 | 143 | 75 | .798 | 1.996 |
| 4888 | 135 | 80 | .988 | 2.470 |
| 4908 | 145 | 80 | .811 | 2.027 |
| 4932 | 137 | 80 | .798 | 1.996 |
| 4956 | 132 | 67 | .834 | 2.086 |
| 4958 | 141 | 69 | .755 | 1.888 |
| 4960 | 134 | 72 | .876 | 2.191 |
| 4978 | 124 | 71 | 1.025 | 2.562 |
| 5100 | 150 | 83 | .809 | 2.024 |
| 5102 | 159 | 88 | .765 | 1.913 |
| 5104 | 147 | 88 | .920 | 2.302 |
| | | | $u_{mean}$=0.898 | $u_{mean}$=2.24 |
| | | | $\sigma$ = 0.139 | $\sigma$ = 0.349 |

1. U values reported in units of $\frac{Btu}{hr\text{-}°F\text{-}ft^2}$

**Figure 4.3.6 Pipe Loss Coefficient Estimation**

The two average u values for the pipe loss of the system are those used for the upper and lower bounds of the TRNSYS runs.

## Heat Exchanger UA Determination

The TRNSYS heat exchanger model enables the user to input either the effectiveness or the overall heat transfer coefficient (UA) product of the heat exchanger. For different operating flow rates of the heat exchanger the effectiveness will vary, but Kays and London state [9] that U can be generally treated as a constant. Thus the approach of using a constant U instead of a constant effectiveness is considered to be more accurate.

The effectiveness of the heat exchanger is calculated for the conditions used to determine the glycol flow rate. Only supply water was sent into the heat exchanger for this condition. The effectiveness of the heat exchanger is 0.69 for these operating conditions (Section 4.3 Glycol Flow Rate). Applying the counterflow Effectiveness-$N_{tu}$ equation [9]:

$$\varepsilon = \frac{1-e^{-N_{tu}(1-C_{min}/C_{max})}}{1-(C_{min}/C_{max})e^{-N_{tu}(1-C_{min}/C_{max})}} \tag{4.10}$$

where $N_{tu}$ is defined:

$$N_{tu}=\frac{UA}{C_{min}} \tag{4.11}$$

these two equations were combined and solved for UA resulting in a value of 609000 (Btu/hr-°F) which has been input to the TRNSYS model.

**Tank to Load Pipe and Ground Losses**

There are approximately 1400 feet of 6 inch ID pipe between the storage tank and the meat packing plant where the energy is calculated and the hot water is used. The pipe is buried eight to ten feet below the surface, well below the freeze line, so ambient conditions do not affect the heat transfer from the line. Energy lost has been attributed to two components; the pipe and the surrounding ground. As a means of estimating an upper limit to this energy lost , the pipe and ground are assumed to begin each day at a temperature of 50°F, and 110°F water is pumped through the pipe.

| | Steel | Soil |
|---|---|---|
| Density $\frac{lbm}{ft^3}$ | 486 | 128 |
| Specific Heat $\frac{Btu}{lbm\text{-}°F}$ | 0.105098 | 0.439 |
| Thermal Conductivity $\frac{Btu}{hr\text{-}ft\text{-}°F}$ | Not Used | 0.3 |

**Figure 4.3.7 Heat Transfer Properties**

The first component is calculated by determining the energy required to heat the pipe (with a 3/8 inch wall thickness) to the steady state temperature of 110°F. Using the material properties for a steel outlined above from Incropera and De Witt [11], the energy to heat the pipe from 50 to 110 °F is about 2 therms.

Next, assuming a constant wall temperature of 110°F, the amount of energy which goes to heating the ground is calculated using a software program called Finite Element Heat Transfer (FEHT) [10]. FEHT enables the user to solve both steady state and transient heat transfer problems by drawing in the mesh (including material properties), setting all boundary and initial conditions, and reducing the mesh size to one which yields a solution. The mesh size is considered small enough when a further reduction in mesh size results in no change in the solution.

The above soil properties were put into the FEHT program for a transient solution and run for a 7 hour simulation. After 7 hours, the temperature distribution in the ground has reached near steady state, so breaking up the ground into 6 concentric rings of approximately constant final temperature surrounding the pipe, the energy into each ring is calculated for the total length of 1400 feet.

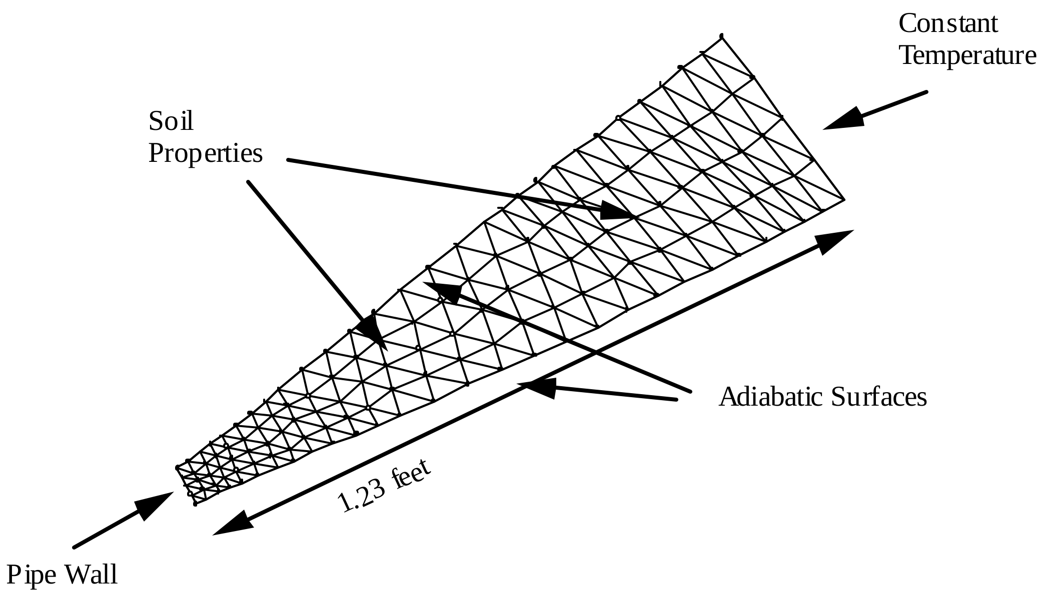


**Figure 4.3.8 FEHT Soil Model**

The results of the FEHT model showed temperatures at various distances outlined in the table below. The energy into each ring is calculated and the sum of the energy into all rings yields an upper limit of the energy required to heat the ground. The following set of equations were solved for the energy into the ground:

| | |
|---|---|
| rho=128 | {lbm/ft^3} |
| Cp=0.439 | {Btu/lbm-F} |
| De=m*Cp*dT/(1e5) | {Therms} |
| m=L*(pi/4)*(d2^2-d1^2)*rho*(1./144.) | {lbm} |

L=1400 {ft}

where d1 and d2 are the diameters (in inches) of each ring of approximate constant temperature. The variable dT is the difference of the soil temperature in the respective ring from the soil starting temperature of 50°F and dE is reported in therms:

| dE | d1 | d2 | dT |
|---|---|---|---|
| 3.988 | 6.750 | 7.923 | 54.000 |
| 4.229 | 7.923 | 9.288 | 41.950 |
| 4.587 | 9.288 | 11.041 | 30.000 |
| 5.060 | 11.041 | 13.690 | 18.000 |
| 4.228 | 13.690 | 17.783 | 7.650 |
| 1.930 | 17.783 | 23.793 | 1.800 |

**Figure 4.3.9 Soil Warming Energy**

The sum of the energy to heat up the soil plus the energy required to heat up the pipe is 26 therms. For each day of operation, this has been used as the energy being lost to the ground. It is considered an upper limit because it is unlikely that the water in the pipe or the surrounding ground cool back down to ground temperature after each day of use. The water provided to the load for this analysis was considered to be a constant 110 °F. Although it will vary throughout the year, it is a reasonable load temperature commonly experienced at Packerland.

**Tank Loss Coefficient**

The storage tank is 41 feet tall with a diameter of 38.3 feet. The top is insulated with 3 inches of sprayed foam, the sides with 3 inches of fiberglass, and the bottom with 2 inches of foam glass. Losses from the tank will be calculated using the top and side insulation to determine the tank loss coefficient ($U_{tank}$) for the TRNSYS model.

The top of the tank has an area of 1152 $ft^2$ and the side 4933 $ft^2$. The parameter $U_{tank}$ is calculated by:

$$U_{tank} = k \frac{\left[\frac{A}{L_{top}} + \frac{A}{L_{side}}\right]}{A_{total}} \tag{4.12}$$

where k is the thermal conductivity of the insulation, $L_{top}$ and $L_{side}$ are the respective insulation thicknesses, and $A_{total}$ is the total top and side area. Using a thermal conductivity of 0.023 $\frac{Btu}{hr\text{-}ft\text{-}°F}$ [11], the value of $U_{tank}$ was found to be 0.10 $\frac{Btu}{hr\text{-}ft^2\text{-}°F}$. This is the value for the tank loss coefficient used in the TRNSYS model.

**Load Determination**

During the eleven day data acquisition period, the total load flow and energy provided for each day is known. Figure 4.3.10 contains this information, and combined with the tank level information, the load profile for the period is constructed. Although there is clearly energy being drawn from the tank during the weekend, the standard practice at Packerland Solar is to report weekend energy supplied on the previous Friday.

| Date | Starting Hours | Water Drawn (Gallons) | Energy Provided (Therms) |
|---|---|---|---|
| July 22 | 4848 | 280896 | 1242.9 |
| July 23 | 4872 | 371072 | 1724.6 |
| July 24 | 4896 | 350848 | 1554.2 |
| July 25 | 4920 | 356032 | 1353.9 |
| July 26 | 4944 | 448576 | 1506.1 |
| July 27 | 4968 | 0.0 | 0.0 |
| July 28 | 4992 | 0.0 | 0.0 |
| July 29 | 5016 | 228800 | 998.6 |
| July 30 | 5040 | 334976 | 1524.3 |
| July 31 | 5064 | 330432 | 1362.7 |
| August 1 | 5088 | 337728 | 1461.6 |
| Total | 264 | 3.039E6 | 12.73E3 |

**Figure 4.3.10 Energy and Water Output**

Constructing the load profile was a matter of considering two occurrences seen in the tank level data. The first is an evening draw. In Figures 4.3.11a and 4.3.11b, the data starts at 12:00 AM, so each major tic mark is a one day period. It can be seen that occasionally there was water drawn from the tank during late evening or early morning hours by the reduction in tank level. Using the tank volume and the times during which the draw occurred, a constant draw was constructed for this time, since there was no replacement water from the system.

The second piece of information used is the total draw for each day of operation. The remaining draw from the tank was at a constant rate over approximate hours of operation of the meat packing plant.  This approach had to be taken since the actual minute to minute load profile is not known.

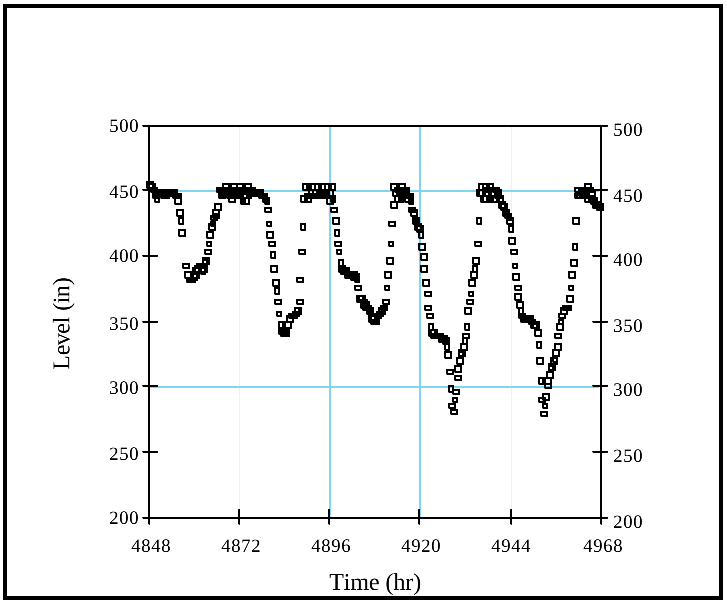


**Figure 4.3.11a Week One Tank Level**

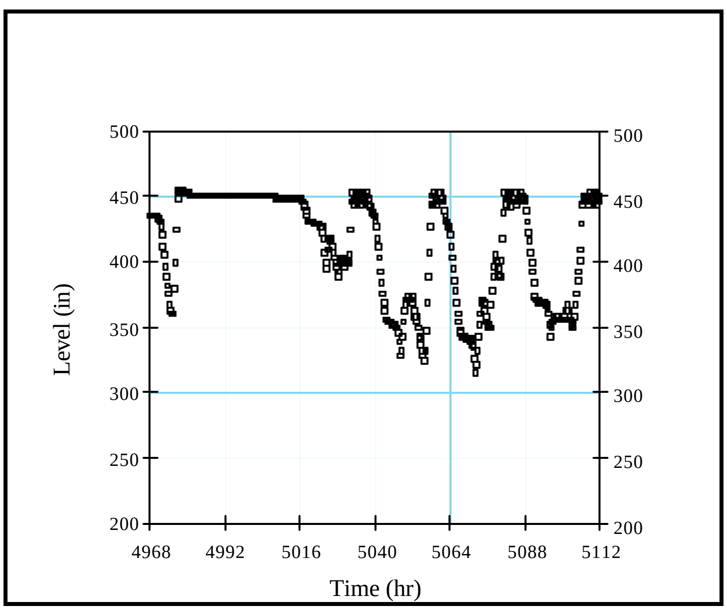


**Figure 4.3.11b Week Two Tank Level**

The load profile is shown in Figures 4.3.12a and 4.3.12b. This profile draws the daily load at a constant rate between the hours of 8:00 AM and 6:00 PM, except where the load was clearly distinguishably different. The profile during each day of operation is varied by the magnitude of the draw rate, and the duration of the draw, always ensuring the total draw for the day matches the actual draw.

The 20 different magnitudes shown in Figures 4.3.12a and b correspond to the load flow rates present in the TRNSYS program in the Appendix. In the equation statement of the program, M1 through M20 are reported in gallons/hour which correspond to the below graphs. Since the actual minute to minute load profile is not known, two variations of the load profile have been generated. These two profiles will be presented and discussed later as well as their effect on the TRNSYS energy output.

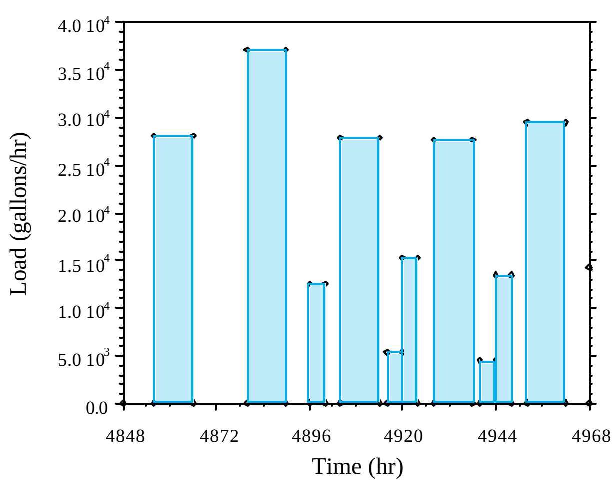


**Figure 4.3.12a Load Profile One, Week One**

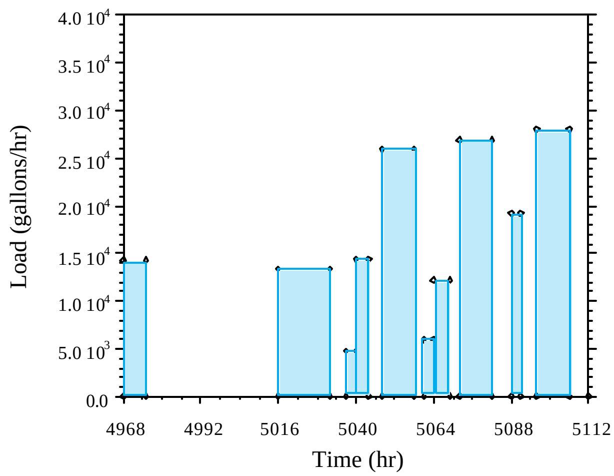


**Figure 4.3.12b Load Profile One, Week Two**

## 4.4 ELEVEN DAY TRNSYS RESULTS

The initial goal of the eleven day TRNSYS model was to verify that the parameters chosen in the previous section would yield an energy output of the system close to the measured output. The eleven day model will then be used to achieve the final goal of the project, which is to make economically feasible changes to the system to improve the energy output. Using Load Profile One, the model was run and the total energy was recorded. Next the load profile was varied slightly to see the effect on energy output, always ensuring that the daily draw of water from the tank was the same as what was actually drawn. The parameter Imin is used in the TRNSYS program to determine when to turn on the glycol pumps and was varied to demonstrate TRNSYS output is not highly dependent on selection of this parameter. The temperature measurements which determined the heat exchanger UA and glycol flow rate were available in integer values of degrees Fahrenheit. An attempt to determine the sensitivity to these measurements is made in this section. The tank to heat exchanger mass flow rate is varied throughout the day in the last sensitivity study as a means of demonstrating the energy output from the TRNSYS model is not highly dependent on it. Finally the results of the eleven day TRNSYS runs are presented.

In the eleven day TRNSYS simulations quite often the change in internal energy (between day 1 and day 11) of the storage tank comprises a significant portion of the energy gathered during this time (on the order of up to 6 percent). The storage tank in TRNSYS automatically calculates the change in internal energy from the beginning to the end of the simulation. As a means of normalizing all eleven day computer simulations and comparing them to the actual energy output of the system during the same time period, the change in internal energy will be added to the energy drawn from the tank. The bulk temperature at the end of the eleven day data acquisition period (see Figure 4.4.6) is approximately 120°F, warmed from an initial temperature of 101°F, resulting in an increase in internal energy of 523 therms.

Load Profile One was determined by assuming a constant draw (aside from the night draw) during the hours of 0800 to 1800. The other two load profiles drew the water between 0900 and 1700, and 0700 to 1900 hours. Using a two node tank model and the low pipe loss coefficient between the collector array and the tank, the following output was calculated.

| Load Profile | Water Drawn (gal) | Energy (therms) |
|---|---|---|
| 1 | 3.039E6 | 1.28E4 |

| | | |
|---|---|---|
| 2 | 3.039E6 | 1.29E4 |
| 3 | 3.039E6 | 1.27E4 |

**Figure 4.4.1 Effect of Load Variation on Energy Output**

Variation of the hours during which water is drawn from the tank have little effect on the energy output. The energy and water output of the plant compare favorably to what the system actually provided as shown in Figure 4.3.10.

The parameter Imin is the minimum radiation seen when the glycol pumps are turned on. The value used for the eleven day simulations was 16 Btu/hr (Section 4.3). The eleven day TRNSYS computer simulation was re-run with Imin values of 5, 30, and 45 Btu/hr as a means of demonstrating the predicted output from Packerland is not highly dependent on the selection of this parameter.

| Imin (Btu/hr) | Energy (E4 therms) |
|---|---|
| 5 | 1.28 |
| 16 | 1.28 |
| 30 | 1.28 |
| 45 | 1.27 |

**Figure 4.4.2 Sensitivity to Imin Selection**

The temperature measurements used to determine the heat exchanger effectiveness, UA, and the glycol flow rate give only integer values in their measurements. Two variations from the measurements taken in Section 4.3 (Glycol Flow Rate) were considered to get an estimate on the error encountered if these measurements were off by one degree each. The two cases were chosen as such as a means of first determining a maximum effectiveness, then a minimum effectiveness, and finding the corresponding UA and glycol flow rate. These values were input into the 11 day model and the results are shown in the below figure.

| | Case 1 | Case 2 |
|---|---|---|
| $T_{c,o}$ (°F) | 75 | 73 |
| $T_{c,i}$ (°F) | 37 | 38 |
| $T_{h,i}$ (°F) | 89 | 91 |
| $\varepsilon$ (ND) | 0.73 | 0.65 |
| UA ($\frac{Btu}{hr\text{-}°F}$) | 664200 | 546000 |
| Q (GPM) | 1400 | 1180 |
| Energy (E4 Therms) | 1.30 | 1.26 |

**Figure 4.4.3 Sensitivity to HX Temperature Measurements**

The ability to increase the tank to heat exchanger mass flow rate was not incorporated into the model. This capability exists in the real system with its three pumps. Normal operation of the system minimizes the number of pumps operating at times of low solar radiation as a means of reducing the pumping costs. The control strategy is quite complicated and often subjective so has not been built into the model. The following graph is an indication that this choice of a constant mass flow rate (all three pumps operating) for all eleven day runs is a reasonable choice, and does not result in a significant difference in the predicted energy output. The pump operating times are shown below, chosen as such to be operating 1, 2, and 3 pumps symmetrically about solar noon. Section 4.3 discusses how the tank to heat exchanger mass flow rates are calculated. These values (2770 GPM with one pump, 3420 GPM with two, and 4500 GPM with three) were input to the eleven day model with the corresponding output. Since the bulk of the energy collected by the system occurs with three pumps on, this is the parameter which predominates in the calculation of energy output. The remainder of the eleven day runs use a constant mass flow rate for the entire day and the respective energy output is shown in Figure 4.4.7.

| 1 pump hours | 2 pump hours | 3 pump hours | Energy (E4 therms) |
|---|---|---|---|
| 0000-0800<br>1800-2400 | 0800-0930<br>1615-1800 | 0930-1615 | 1.29 |
| 0000-0730<br>1830-2400 | 0730-0900<br>1645-1830 | 0900-1645 | 1.28 |
| 0000-0830<br>1730-2400 | 0830-1000<br>1545-1730 | 1000-1545 | 1.28 |

**Figure 4.4.4 Hours for Pump 1 Variable Mass Flow Rate**

For Load Profile 1, Imin equal to 16, constant daily heat exchanger to tank mass flow rate (4450 GPM) and a heat exchanger UA of 609000 the daily energy output has been tabulated and presented in Figure 4.4.5, compared to the energy output from the system on the same days. The weekend output is reported on Friday as is the Packerland output. Although the daily energy output fluctuates between the two, the sum energy output for the two is very close, as can be seen on Figure 4.4.7 where the X occurs (1.268 E4 plus the change in internal energy of 523 therms).

26 therms for 9 load days (234 therms total) have been subtracted from each of the TRNSYS day totals to yield Figure 4.4.5. Figure 4.4.5 presents the results of what is

considered the best TRNSYS run for the eleven day period during which time a total of 1.23E4 therms were computed.

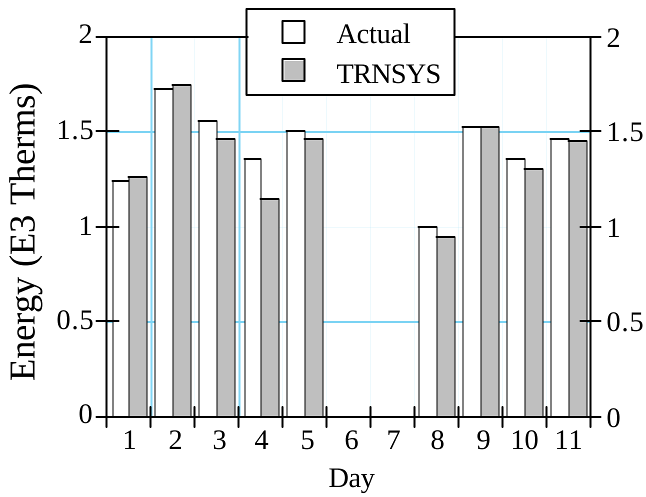


**Figure 4.4.5 Daily Energy Comparison**

The TRNSYS tank temperatures in the top and bottom, for Load Profile 1, have been compared to the actual tank temperatures recorded at the 2 and 25 foot level during the same time period. During the entire 11 day period the temperatures in the TRNSYS model clearly follow the actual tank temperatures (Figure 4.4.6). This information, along with very similar energy output and nearly identical draws from the tank, indicate the model produces results very close to those of the actual system.

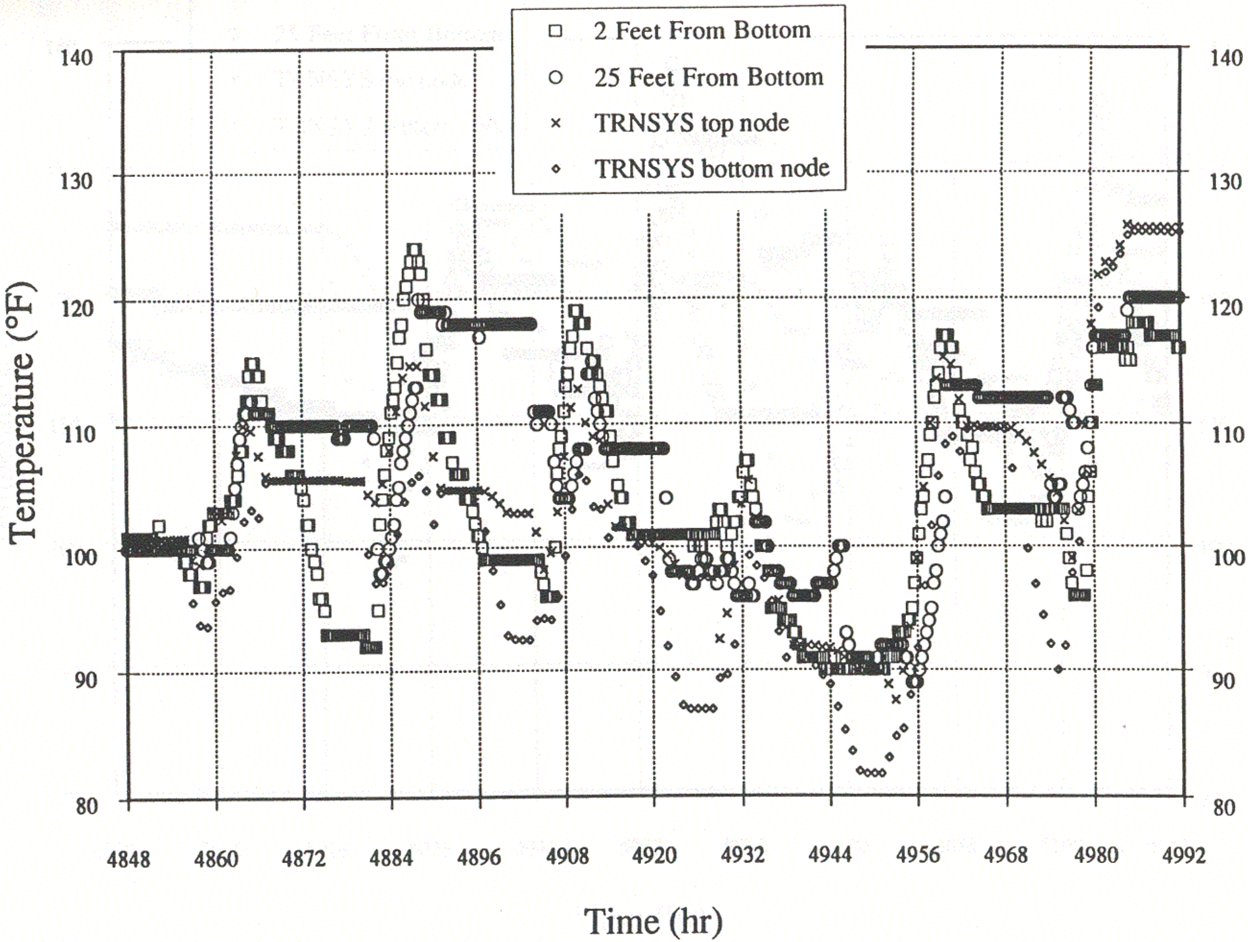


**Figure 4.4.6a Tank Temperatures**

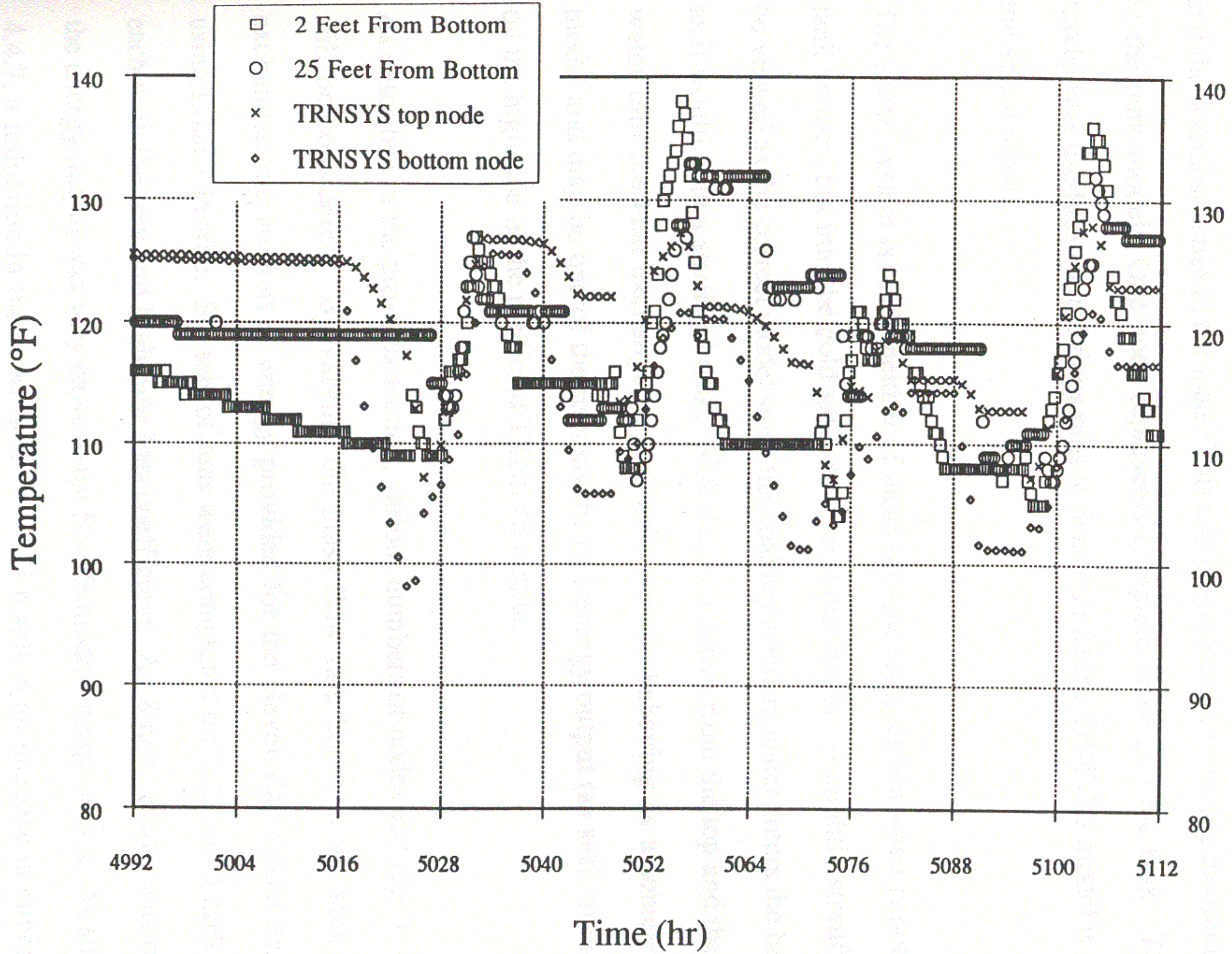


**Figure 4.4.6b Tank Temperatures**

Stratification in the tank, when accompanied by drawing from the tank bottom to the heat exchanger and the tank top to the load, will send the coldest water to the heat exchanger and the warmest water to the load. This can be modeled by varying the number of nodes in the tank model. One node represents complete mixing in the tank. The two node model was used for the previous runs to demonstrate the TRNSYS model is very close to the actual model.

The actual system is really neither of these because replacement water is not sent into the tank bottom, but into the cold side of the heat exchanger. A slightly stratified tank may be viewed as the correct model since the cold replacement water enters the heat exchanger as it would with a stratified tank. With the load drawn from the top and the replacement water into the heat exchanger, the system may be behaving as a somewhat stratified model and may be one of the reasons the true energy output (as seen in Figure 4.4.7) is on the high side of the predicted TRNSYS output.

As described in the previous section, various numbers of nodes and pipe loss coefficients will be considered. By varying the mass flow rate between the tank and the heat exchanger, the amount of energy provided for the eleven day model has been varied using Load 1 Profile. Six sets of runs were completed for 1, 2, and 5 node tank models, each with the low and high pipe loss coefficient. An 8 node model was run as well but the energy output was very close to the 5 node model energy output. As shown in Figure 4.4.7, a reduction in the mass flow rate will result in an increase in energy output only when accompanied by tank stratification. For a completely mixed tank, a reduction in the mass flow rate will reduce the energy output.

The X on the figure is where the actual system energy output is using true system parameters. Again, for each of the TRNSYS runs, a total of 26 therms per day (for 9 days of draw) or 234 therms have been subtracted from the TRNSYS output as a means of representing the thermal losses to the ground between the tank and the load.

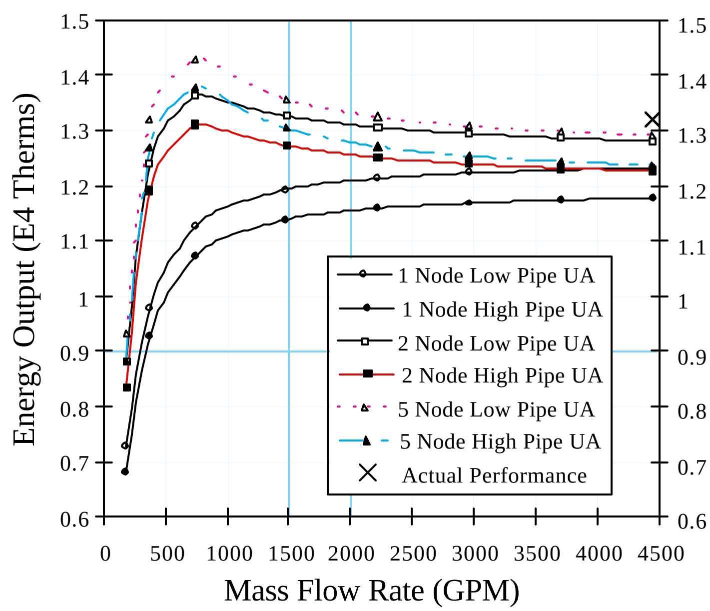


**Figure 4.4.7 Eleven Day Energy Output**

## 4.5 ANNUAL SIMULATION RESULTS

An annual simulation was set up using the Weather Generator (TYPE 54) in conjunction with the Solar Radiation Processor (TYPE 16) using the TRNSYS model developed in the previous section,. The Weather Generator [19] generates hourly weather data given the monthly average values of solar radiation, dry bulb temperature, and humidity ratio [20]. Hourly horizontal radiation are generated using Type 54. Type 16 enables the TRNSYS user to use a variety of correlations which break the total horizontal radiation into its beam and diffuse components, and project it onto the tilted collector surface [19].

The Boes et al. correlation was used for the Horizontal Radiation Mode, and the Isotropic Sky Model used for the Tilted Surface Radiation Mode. The 1990 load data was used for the annual simulation along with an effective number of collector panels of 4978 (as discussed in Section 4.1). During this year there were 260600 therms provided to the meat packing plant with a load flow of 68.08E6 gallons of water. For the actual flow rates of the glycol and tank side water, and the low pipe loss coefficient previously discussed, the annual simulation predicted an energy output of 235900 therms. The Reindl (reduced) correlations were used in place of the Boes et al./Isotropic Sky Models to verify the energy output is not highly dependent on the Horizontal or Tilted Surface Radiation Modes. For the same load flow from the tank for the year, the annual predicted energy output was 244600 therms, or 2.2 percent different.

The load was not drawn at a constant rate over the year as in the *f*-Chart simulations. Instead, a sinusoidal draw occurring over the 12 month interval was constructed to draw the maximum load in the month of July, and the minimum in the month of January. For 1990 the total annual draw was 68.08E6 gallons of water. If this were drawn only on weekdays, the average draw for the day would be 261000 gallons, or for a 10 hour draw period, 26100 gallons per hour. For the peak summer draw, during the month of July the maximum hourly draw was set to an average of 42000 gallons per hour, resulting in a ratio of 1.6084 with the average hourly draw. This peak load varied sinusoidally results in a ratio of 0.3916 which occurs in January. Intermediate monthly ratios are shown in Figure 4.5.2. The resulting total load flow is also presented in the table. This was the profile used for all of the annual simulations, the results of which will be presented later in this section.

To demonstrate the annual output of the system is not highly dependent on the selection of the amplitude of the sinusoidal variation of the annual load profile, two other amplitudes of the annual load flow were selected and run with the same system parameters and radiation as presented above (Boes et al. Horizontal and Isotropic Sky Tilted Radiation Models). The second profile results in a maximum hourly draw of 50400 gallons, the third in a maximum hourly draw of 34060 gallons, with the maximum always occurring in July.

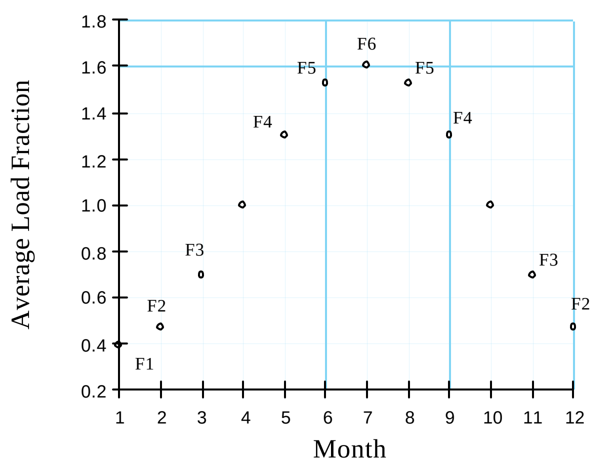


**Figure 4.5.1 First Profile Load Variation**

As can be seen in Figure 4.5.2, the annual energy output does not vary significantly for a widely varying type of load profile.

| | First Profile | Second Profile | Third Profile |
|---|---|---|---|
| F1 | 0.3916 | 0.0699 | 0.6597 |
| F2 | 0.4731 | 0.1945 | 0.7053 |
| F3 | 0.6958 | 0.5350 | 0.8299 |
| F4 | 1.3042 | 1.4650 | 1.1702 |
| F5 | 1.5269 | 1.8055 | 1.2947 |
| F6 | 1.6084 | 1.9301 | 1.3403 |
| Total Draw (E6 Gall) | 68.14 | 68.28 | 68.04 |
| Energy (E5 Therms) | 2.359 | 2.302 | 2.339 |

**Figure 4.5.2 Annual Sinusoidal Load Variation**

The first profile was used for the annual runs which are presented in Figure 4.5.3. The X on the plot represents the actual energy output for 1990 of 260600 therms. Although considerably higher than the predicted energy output for the same load conditions, it is for a solar profile generated with the TRNSYS Weather Generator and not actual solar data as was used for the 11 day simulations. For the annual simulations the trend in the energy output clearly follows that of Figure 4.4.7. Again, for a reduced mass flow rate between the storage tank and the heat exchanger an increase in the energy output can be expected due to taking advantage of the increased stratification within the tank.

The $f$-Chart method does not take advantage of the thermal stratification within the tank. It is a simple method which has the intention of providing easy to acquire estimates on the energy output for a solar system. Subtracting the energy lost to the ground from the 1990 $f$-Chart results (constant incidence angle modifier) we see an energy output of 226000 therms. Although this does not compare as favorably to the actual energy output of 260600 therms as might be desired, again it must be remembered that this energy output is based on average weather data (as is the TRNSYS results), not on actual data. It does, on the other hand, provide a fairly close estimate to the energy output (based on the same monthly weather data) as the TRNSYS output.

6760 therms were subtracted from each of the annual TRNSYS and *f*-Chart results as a means of representing the energy lost to the ground as previously discussed. 6760 therms are calculated from 26 therms per day for 52*5 operating days of the year. This was not subtracted from the *f*-Chart energy reported in Figure 4.1.2 but has been for this comparison.

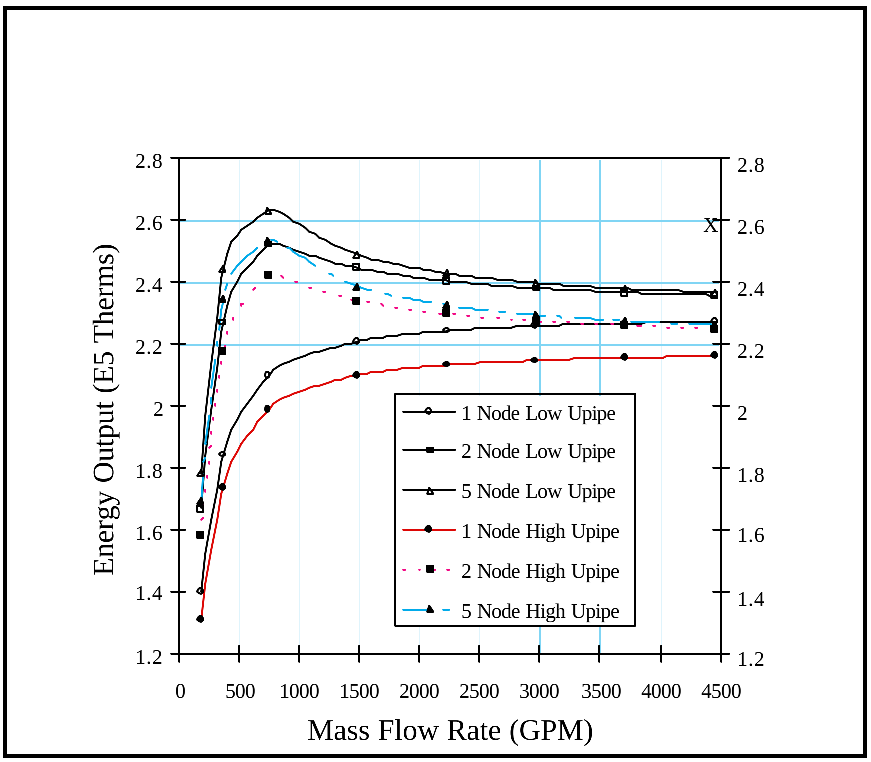


**Figure 4.5.3 Annual Simulation Energy Output**

## 4.6 CONTROL STRATEGY EVALUATION

The current control strategy is designed to not only keep the maximum flow rate between the tank and heat exchanger, but also to lower the tank level in the morning and the evening so the very cold supply water can be input directly to the heat exchanger (during low levels of solar radiation). Originally the system was built to draw the load off of the tank top and the heat exchanger water from the bottom, but for this system of operation the tank level could not be varied since the outlet to the load was fixed. The piping was re-worked [12] to enable the tank level variation. Clearly there is a benefit to being able operate during lower levels of radiation, and removing the energy from the hot glycol at the end of the day, but there is a cost to this mode of operation as well. This section will evaluate the benefits and costs of these two control strategy approaches.

The first approach used will consider the final glycol temperatures at the end of each day experienced in the actual system, and compare them to the final glycol temperatures experienced at the same time using the best case scenario (5 node tank model, 450 GPM tank/heat exchanger flow rate, low pipe UA) see Figure 4.4.7. The current control strategy draws the load from the tank bottom, not taking advantage of the benefits of thermal stratification. The cost is a reduction in energy output due to more tank mixing, with a benefit of being able to remove the energy from the glycol at the end of each day. As a means of comparing these two strategies the final glycol temperatures (actual) are compared to what could have been achieved under a best case scenario (the highly stratified model). The 11 day model is used because TRNSYS temperatures obtained can be directly compared to actual temperatures in the array at the same time during the simulation. The difference in final glycol temperature for each day along with the mass of the glycol in the system and its specific heat yield the amount of energy that could have been removed from the glycol under the current strategy at the end of each day of operation.

| Time (hr) | $T_{g,TRNSYS}$ (°F) | $T_{g,a}$ (°F) | ΔT (°F) | $E_{eq}$ (therms) |
|---|---|---|---|---|
| 4869 | 91.4 | 79 | 12.4 | 25.4 |
| 4893 | 87.5 | 67 | 20.5 | 42.0 |
| 4917 | 98.4 | 62 | 26.4 | 54.1 |
| 4941 | 77.0 | 64 | 23.0 | 47.2 |
| 4965 | 86.6 | 65 | 21.6 | 44.3 |
| 4989 | 94.0 | 106 | -12.0 | 0.0 |
| 5013 | 80.7 | 63 | 16.3 | 33.4 |
| 5037 | 90.7 | 70 | 20.7 | 42.4 |
| 5061 | 94.4 | 68 | 26.4 | 54.1 |
| 5085 | 94.4 | 77 | 17.4 | 35.6 |
| 5109 | 87.2 | 73 | 14.2 | 29.1 |

**Figure 4.6.1 Additional Energy Output**

Under the current mode of operation the glycol is being cooled to lower temperatures at the end of each day when compared to the best case TRNSYS model. Hour 4989 will be considered an unusual day, apparently the control strategy did not function that day for some reason as can be seen in a final glycol temperature of 106°F. For the other 10 days of operation there were a total of 407.6 therms provided. Assuming that the average (40.76 therms) could have been removed from the glycol at hour 4989 as well, a total of 448.4 therms have been removed from the glycol.

During the 11 day period the amount of energy provided to the plant was 12680 therms. Looking at Figure 4.4.7, the X is where 12680 therms is along with the 523 therms change in tank internal energy. Perhaps the strategy of removing the energy at the end of each day is one reason the actual provided energy is on the high side of the simulation results. This 448.4 therms of energy represents 3.5 percent of the energy provided by Packerland Solar.

The second means of estimating the additional energy output is by performing the same type of analysis for the annual simulation. Using the 2 node, low pipe UA, and actual flow rate (4450 GPM) the glycol temperatures were recorded in a file at the end of each day of operation when the glycol pumps shut down. In Figure 4.6.1 it can be seen that the current control strategy cools the glycol to around 60 to 70°F each day. It was assumed that the glycol at the end of each day could have been cooled from the shut down temperature to 65°F after each day. The sum of the daily totals was 16000 therms for the annual simulation. The total energy provided at Packerland for the same year was 260600 therms and the predicted energy output for this year was 235900 therms. The current control strategy apparently contributes a significant amount of energy to the output of the Packerland system.

The annual simulation predicts that under the current mode of operation about 6 percent of the energy output is due to the control strategy which cools the glycol at the end of each day to extract its energy. The evaluation for the year was performed using the actual flow rates and the system actual system parameters outlined in Section 4.4. The eleven day evaluation was performed using what is considered the best case operating mode, that is, a reduced flow rate between the tank and heat exchanger with a high degree of thermal stratification. As would be expected, since the high degree of stratification sends the coolest water to the heat exchanger, the additional energy output of the system by cooling the glycol is lessened to about 3.5 percent.

Comparison of these results will be discussed in Chapter 5. An attempt will be made to quantify the two modes of operation and determine an optimal control strategy which could take advantage of both the low flow rate/tank stratification potential of the system, as well as the ability to remove energy from the hot glycol at the end of each day of operation.

---

# CHAPTER
# FIVE

# CONCLUSIONS

The goal of this project was to recommend economically feasible system changes to improve energy output at Packerland Solar. The two considerations used to evaluate potential system changes are the flow distribution in the large banks of collectors, and the operational strategy currently employed. The results of both considerations along with additional savings which may be experienced with the implementation of these recommendations are the subject of this chapter. Finally some recommendations for future work in the analysis of large liquid solar collector arrays are discussed.

## 5.1 FLOW DISTRIBUTION

The total glycol flow rate is considerably below the original design flow rate of about 0.85 GPM per collector. It was selected due to recommendations in the product literature provided by the manufacturer. The actual flow rate of 1250 GPM for 5256 collectors is an average of 0.238 GPM per collector. The effect of both the reduced flow rate and the poor flow distribution can be seen in Figure 2.5.2. Nine collectors connected in parallel result in essentially no reduction in performance relative to the ideal case. The effect of connecting 15 collectors in parallel results in approximately a three to four percent reduction in performance, depending on the total bank flow rate.

Assuming the entire collector array experiences the average flow rate, the total system reduction in performance is found by weighting the 1890 collectors connected in banks of 15 with the rest of the array connected in banks of 9. Each bank of 15, at 0.238 GPM average collector flow rate, experiences an approximate four percent reduction in performance. Combined with negligible reduction in performance in the banks of 9 results in a total system reduction in performance of 1.4 percent.

To reduce this loss in the system the 126 banks of 15 collectors would have to be re-piped between the seventh and eighth collectors to make the flow more uniform. Based on the energy output of the system of the last few years, this re-piping would result in an extra 3600 to 4300 therms per year. At an approximate payment of $0.20 per therm since 1987, this represents an additional annual income of between $720 and $864. Considering the probable cost of materials and labor to perform the re-piping of these banks, it appears not feasible to further consider changes in the collector array. If, however, the price per therm paid to the plant were to increase dramatically, it may justify the capital expenditure for the additional energy output.

## 5.2 FLOW RATE AND CONTROL STRATEGY

Considering the results of the flow distribution study, two components which affect the performance of the collector arrays could be improved by: 1) improving the flow distribution in the large banks so the performance approaches the ideal curve (section 5.2), and 2) increasing the overall glycol flow rate to the design flow rate of 0.85 GPM per collector.

However, the goal of this project is to make *economically feasible* changes to the Packerland system. Not only is it unfeasible to consider boosting the pumping power to obtain design flow rates (which probably has practical limitations as well), it may be unnecessary as well.

Hirsch [5], Wuestling [21], and others have discussed the benefits of operating at reduced collector flow rates. There are two opposing effects of reducing the collector flow rate. As seen in Figure 2.5.1 the collector performance is reduced which is the result of viewing the collector bank by itself, not taking into account the effect of the reduced flow rate in conjunction with a very large storage tank with a large capacity for thermal stratification. A highly stratified storage tank enables drawing the load from the (hot) tank top and the heat exchanger inlet from the (cold) tank bottom (see Figure 5.2.1). Wuestling [21] determined that the optimum flow rate occurs at about 20 percent of conventional flow rates. The benefits of this trade-off can be seen in Figures 4.4.7 and 4.5.3. Instead of considering varying the working fluid flow rate in the collector array (Hirsch and Wuestling), the tank to heat exchanger flow rate is varied for this study. In the Packerland case, the optimum occurs with adjustment of this flow rate down to around 400 to 800 GPM.

Referring to Figure 4.4.7, the energy output for the 11 day period is on the high side of the predicted energy output from the TRNSYS model. As discussed in Section 4.6, it may be on the high side due to the control strategy which enables the energy in the glycol to be removed at the end of each day. Removing the energy from the glycol at the end of each day results in approximately 3.5 to 6 percent additional energy being removed from the system. It was calculated by comparing final glycol temperatures in the actual system to the final glycol temperatures which could have been obtained under the more conventional control strategy, and a highly stratified tank. Figure 4.4.7 indicates the current means of control is not without cost. Had the tank to heat exchanger mass flow rate been reduced to the optimum during this time of operation, perhaps an additional 10 percent energy output may have been experienced. The additional energy output is predicted only when operating with a highly stratified tank, and while drawing the load from the tank top.

The original design of drawing the load from the tank bottom was re-worked to enable variation of the tank level to remove energy remaining in the glycol after each day of operation [12]. As a means of benefiting from both these operational strategies, re-furbishing the tank outlet to the load with a floating device which would maintain the inlet to the pipe a few feet below the water surface, would allow Packerland Solar to take advantage of a high degree of thermal stratification within the tank while operating under the current method of varying the tank level and removing late afternoon energy. In this way the system would operate most efficiently while taking advantage of both operating philosophies. With a considerably reduced mass flow rate between the tank and heat exchanger, it would need to be determined if sufficient thermal stratification may be achieved without the use of a manifold at the return from the heat exchanger.

The alternate tank design below is drawn as a means of representing an operation which could take advantage of the variable volume operating philosophy while always drawing the load from the tank top. It would very likely have practical problems which would need to be overcome, such as restricting the movement of the floating device. These problems will not be addressed here. However the general idea can be seen in the drawing.

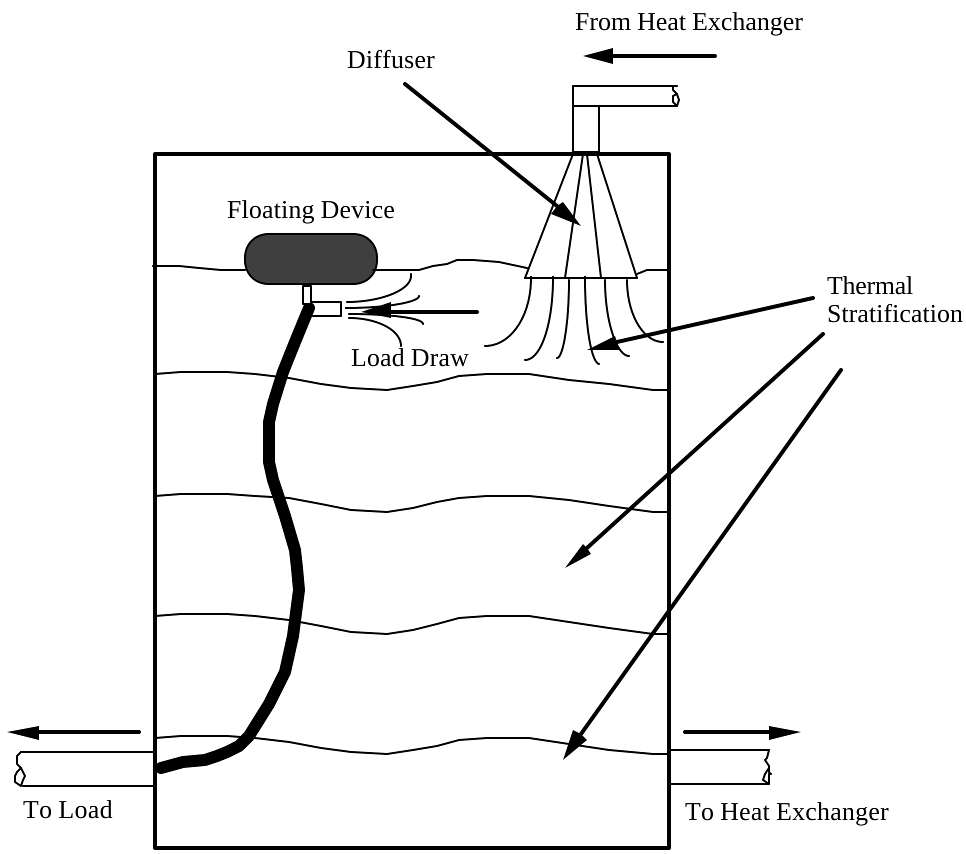


**Figure 5.2.1 Alternate Tank Design**

The range of the potential improved system output was purposely kept vague (10-12 percent). The TRNSYS model cannot be expected, due to some of the built in simplifications, to yield exact results under full annual operation. A certain amount of extrapolation takes place in moving from the 11 day model to the full year but an attempt has been made at justifying these simplifications with the use of the sensitivity studies presented in Chapter 4. In both the 11 day and the annual models, the trend in the improvement is apparent. A reduced tank to heat exchanger flow rate accompanied by thermal stratification in the tank will have a marked difference on the energy output at Packerland Solar.

In addition to the increased energy output which may be seen with the reduced tank to heat exchanger mass flow rate, an additional savings would result from the reduced pumping requirements. Each 10 HP pump equates to 7460 or 7.46 kW. For each hour of operation, at $0.07 per kW-hr, the cost of operating each pump is $0.52. For all three pumps in the tank to heat exchanger loop, this is a cost of $1.56/hour which could be considerably reduced by sending only supply water to the cold side of the heat exchanger. Equating this pumping cost to therms of energy provided by hot water to the meat packing plant, 10 hours of pumping cost approximately $15, or an equivalent of 75 therms of hot water (at $0.20 per therm). During the 11 day simulation, an equivalent of 825 therms of energy, or about 6.5 percent of the energy provided was lost to these pumps alone. Of course this is only an approximation to what was spent during this time, but it is an indication that a considerable percentage of energy output is spent in these pumping requirements.

The recommendations here are issued with a word of caution. Without monitoring system efficiency over extended periods of time by use of a pyranometer on the collector tilt, the benefits of any changes implemented at Packerland Solar cannot be fully evaluated. During the 11 day simulation period, integration of the solar radiation recorded by the tilt pyranometer resulted in a total of 18260 Btu/ft$^2$ of collector area. For 165564 ft$^2$ of collector area, 3.023E9 Btu, or 30230 therms of solar radiation fell on the collector surface. In this time 12680 therms of energy were provided to the meat packing plant and 523 additional therms ended up in the storage tank as internal energy, resulting in a system efficiency of 43.7 percent. The efficiency will certainly vary throughout the year as the system performance will be reduced during the cold weather months, but it is a reference point from which summer system comparisons can be made.

During the annual TRNSYS runs a total of 4.687 therms fell on each square foot of area. With an effective number of collectors of 4978 at 31.5 $ft^2$, the system performed with an efficiency of 32.1 percent (based on the two node model). Under optimal conditions of operation, TRNSYS predicts Packerland could have output approximately 10 percent higher than under the current system of operation. Based on the five node, low pipe UA simulation, the actual energy output may have been as high as 263000 therms (Figure 4.5.3) for the year resulting in an annual efficiency of 35.8 percent.

## 5.3 FUTURE WORK

A starting point for future work in the area of flow distribution should begin by acquiring pressure drop specifications from the manufacturer, and running the SERI program (a copy of which is provided with the master copy of this thesis) to determine the flow distribution. Next the method described in Chapter Two should be implemented with a $K_e$ value of 37.5. If the value of 37.5 is to be considered universal for this type of collector, it would need to be applied to a wide range of collector geometries, and a wide number of collector configurations.